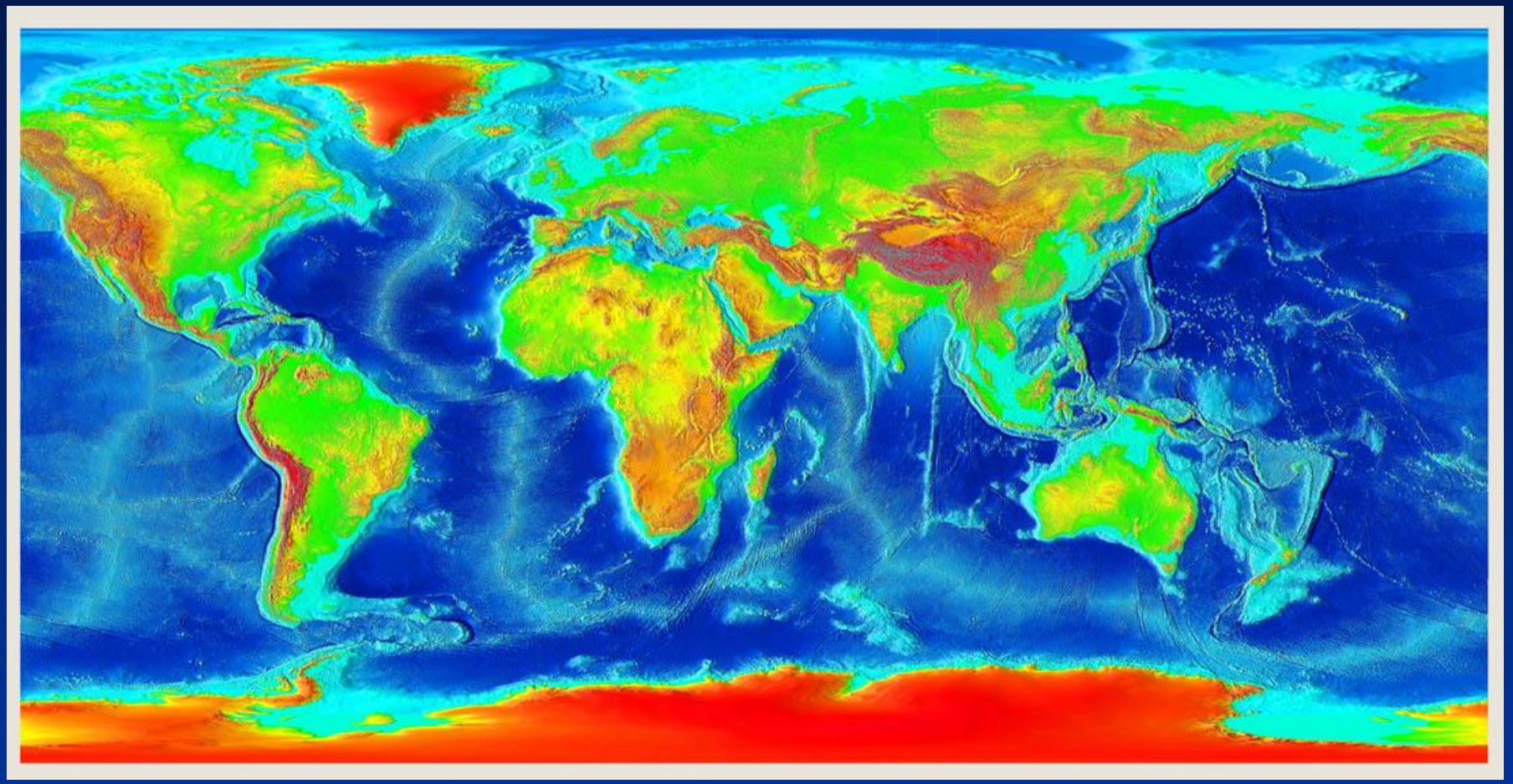

Shaded reliefs e batimetria da NOAA National Centers for Environmental Information (NCEI)

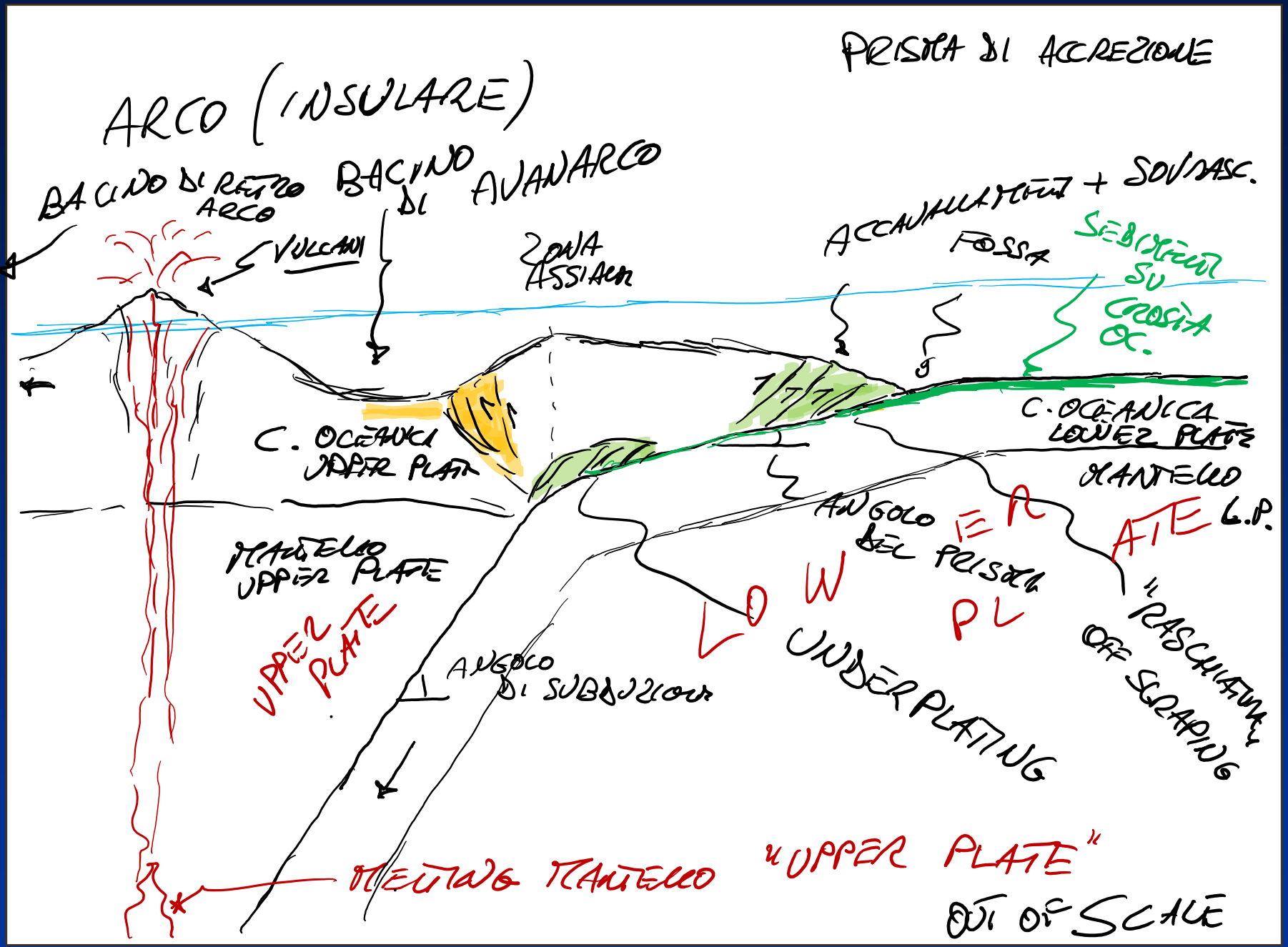
PRISMA DI ACCREZIONE
ARCO (INSULARE)
BACINO DI RETRO ARCO
VULCANI
BACINO DI AVANARCO
ZONA ASSIALE
ACCAVALLAMENTI + SOVRASC.
FOSSA
SEDIMENTI SU CROSTA OC.
C. OCEANICA UPPER PLATE
C. OCEANICA LOWER PLATE
MANTELLO UPPER PLATE
MANTELLO L.P.
ANGOLO DEL PRISMA
UPPER PLATE
LOWER PLATE
UNDERPLATING
"RASCHIATURA" OFF SCRAPING
ANGOLO DI SUBDUZIONE
MELTING MANTELLO
"UPPER PLATE" OUT OF SCALE

Shaded reliefs e batimetria da NOAA National Centers for Environmental Information (NCEI)

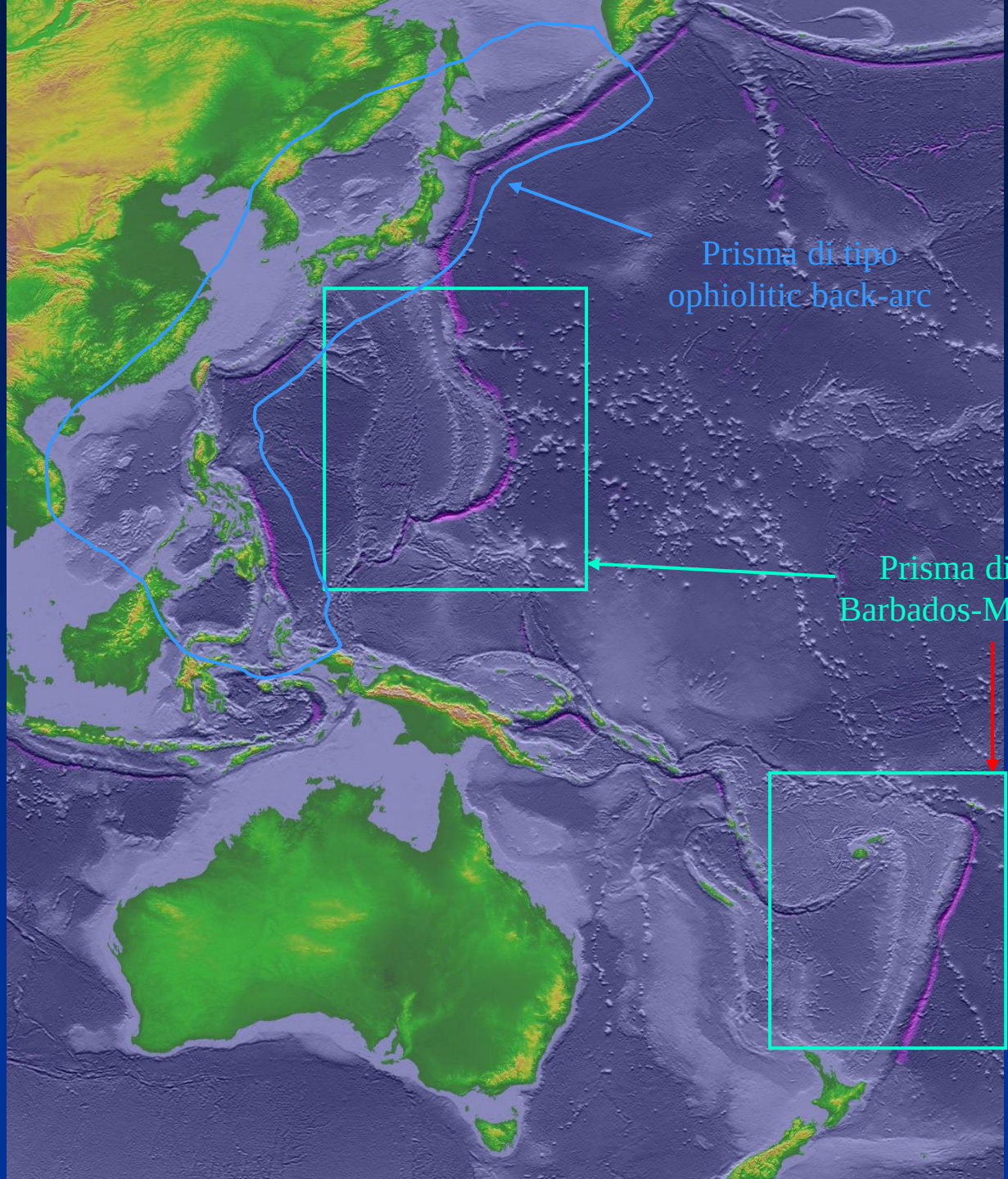

Shaded reliefs e batimetria da NOAA National Centers for Environmental Information (NCEI)

Zona di subduzione delle Piccole Antille - Barbados

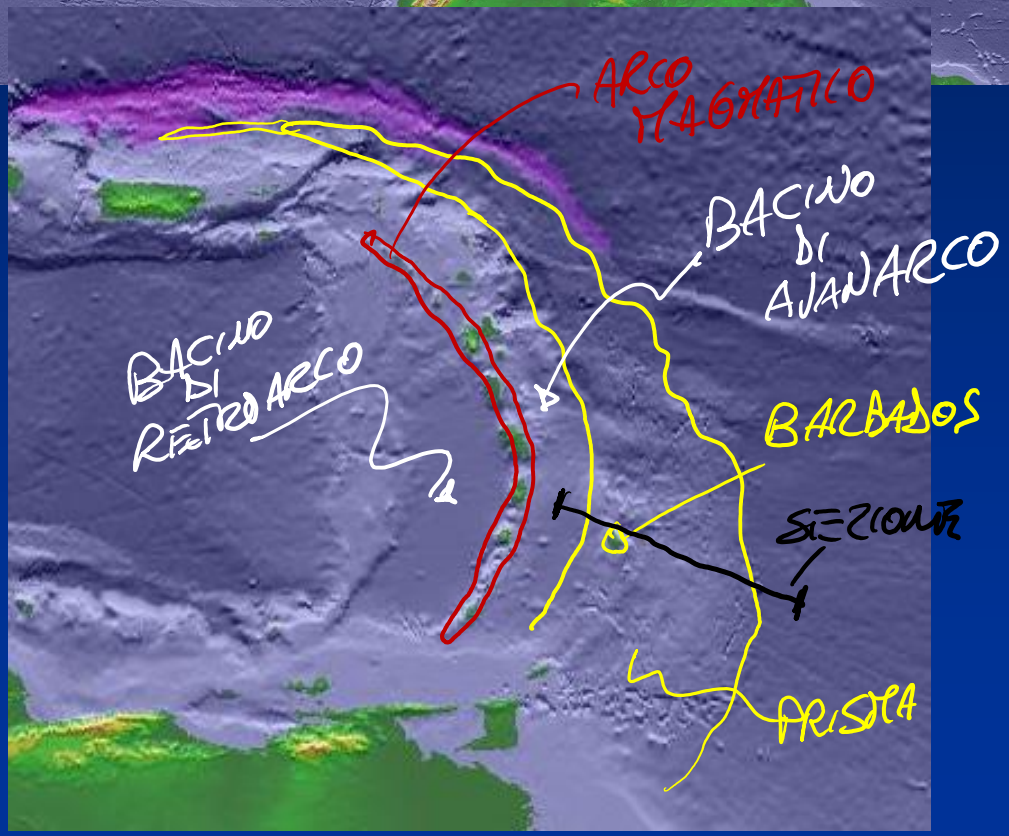

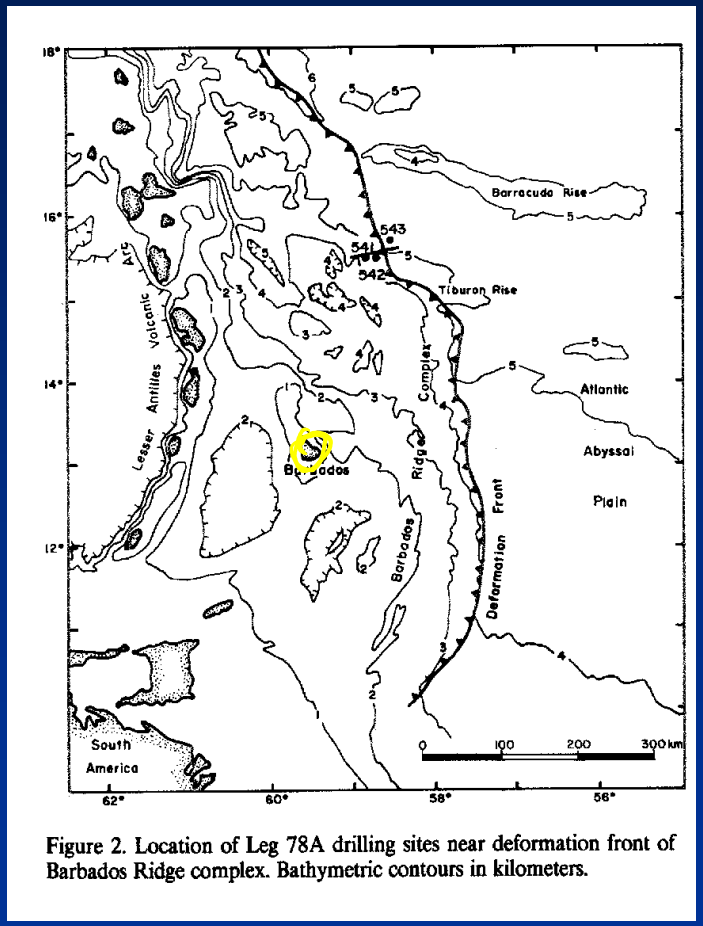

Figure 2. Location of Leg 78A drilling sites near deformation front of Barbados Ridge complex. Bathymetric contours in kilometers.

Moore and Lundberg, 1986

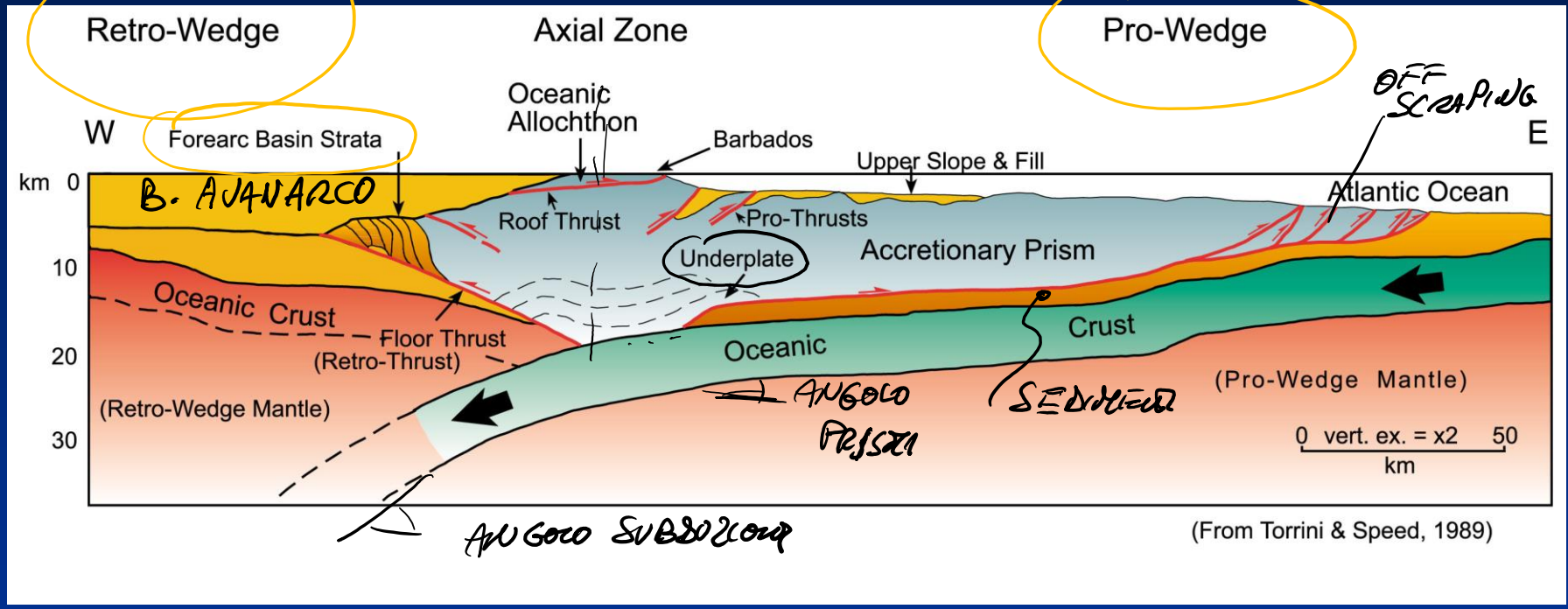
Retro-Wedge
Axial Zone
Pro-Wedge
W
E
Forearc Basin Strata
Oceanic Allochthon
Barbados
Upper Slope & Fill
Atlantic Ocean
km 0
10
20
30
Roof Thrust
Pro-Thrusts
Underplate
Accretionary Prism
Oceanic Crust
Floor Thrust
(Retro-Thrust)
Oceanic
Crust
(Retro-Wedge Mantle)
(Pro-Wedge Mantle)
0 vert. ex. = x2 50
km
(From Torrini & Speed, 1989)

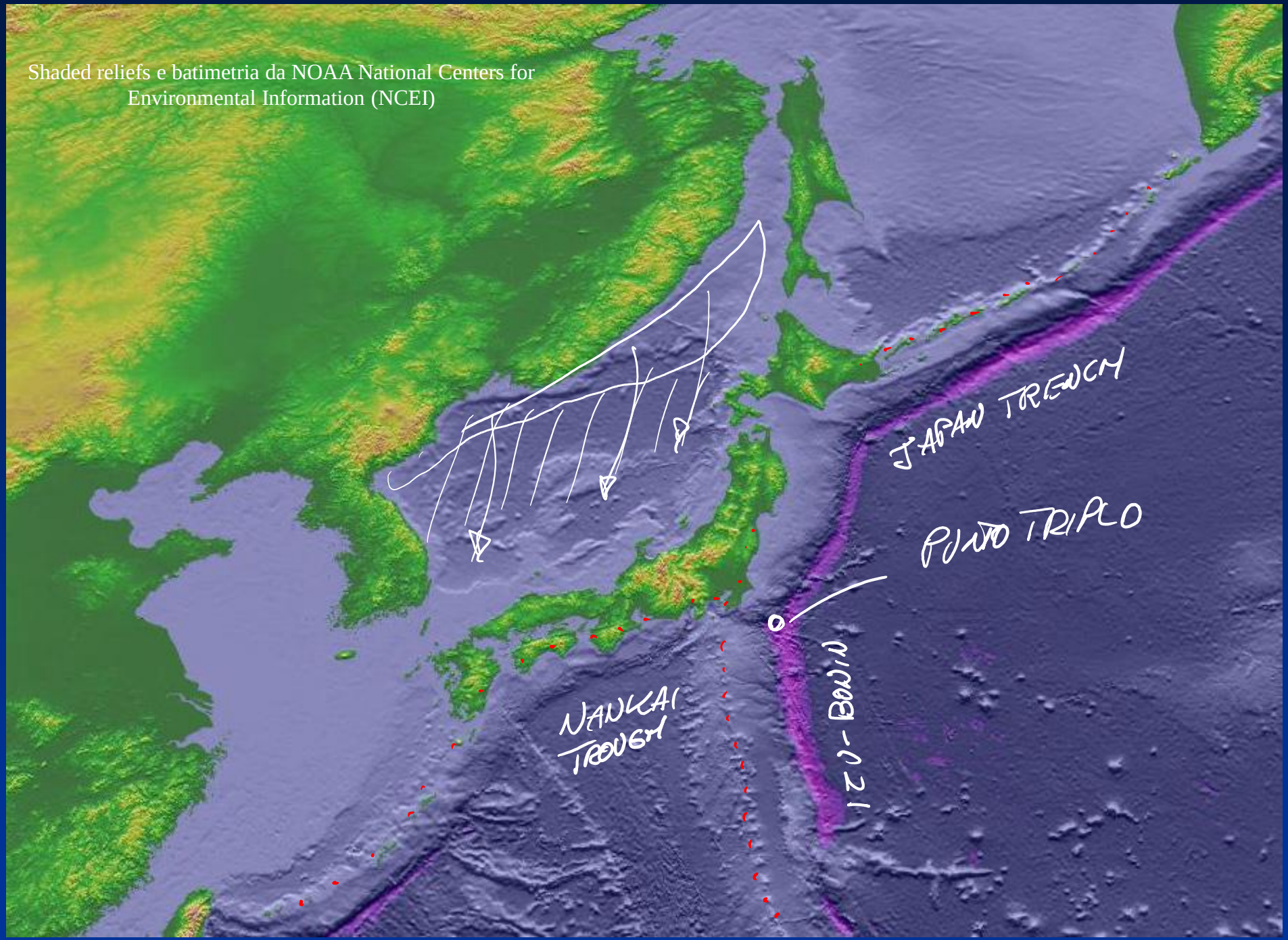
Shaded reliefs e batimetria da NOAA National Centers for Environmental Information (NCEI)
JAPAN TRENCH
PUNTO TRIPLO
NANKAI TROUGH
IZU-BONIN

Laurent Jolivet, Sorbonne Université, CNRS-INSU

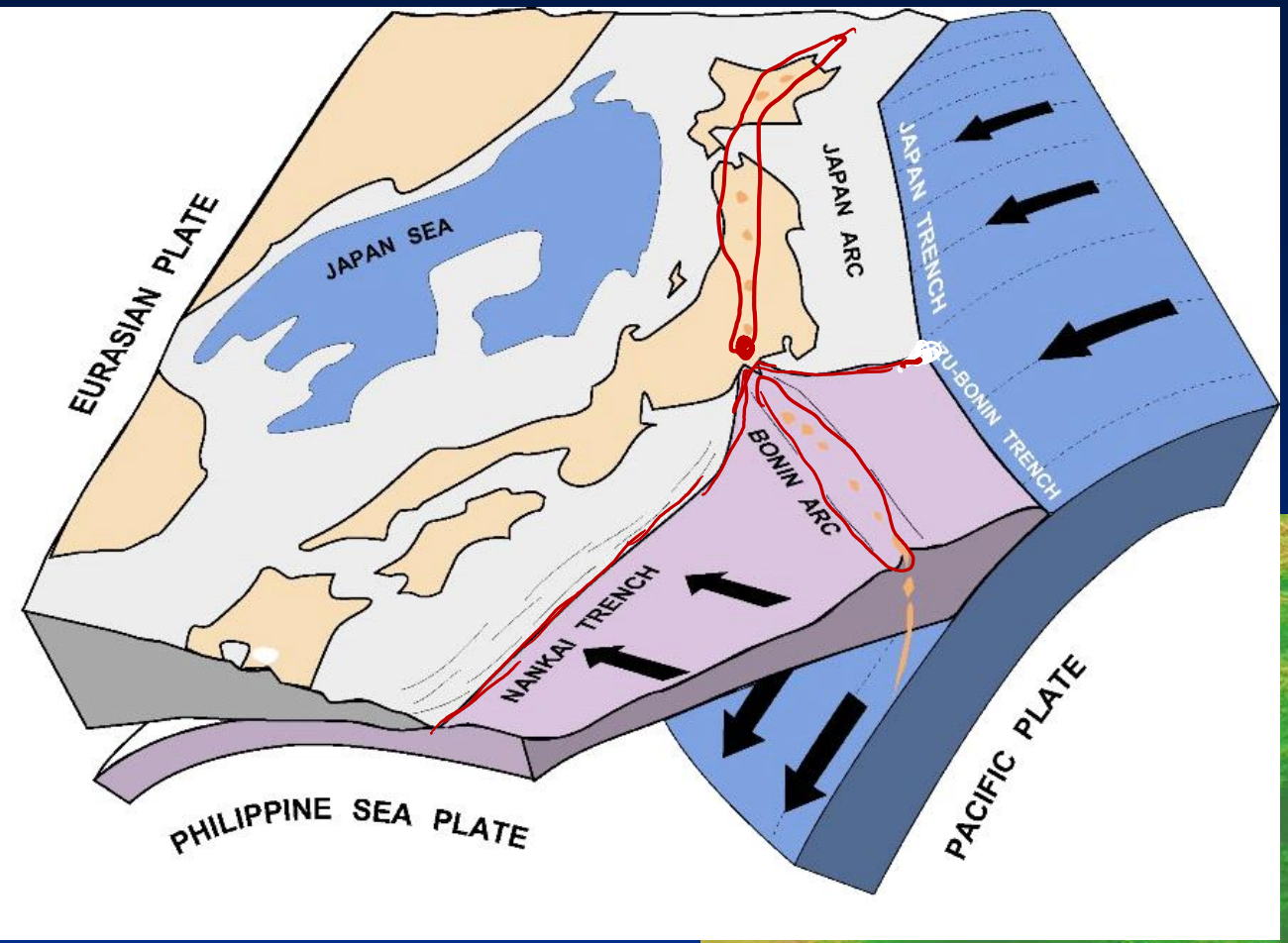

Shaded reliefs e batimetria da NOAA National Centers for Environmental Information (NCEI)

Figure F1. Map showing locations of Leg 190 and 196 sites. The red box outlines the location of the three-dimensional seismic survey. Yellow numbers indicate sites revisited during Leg 196. Depth contours are in kilometers.

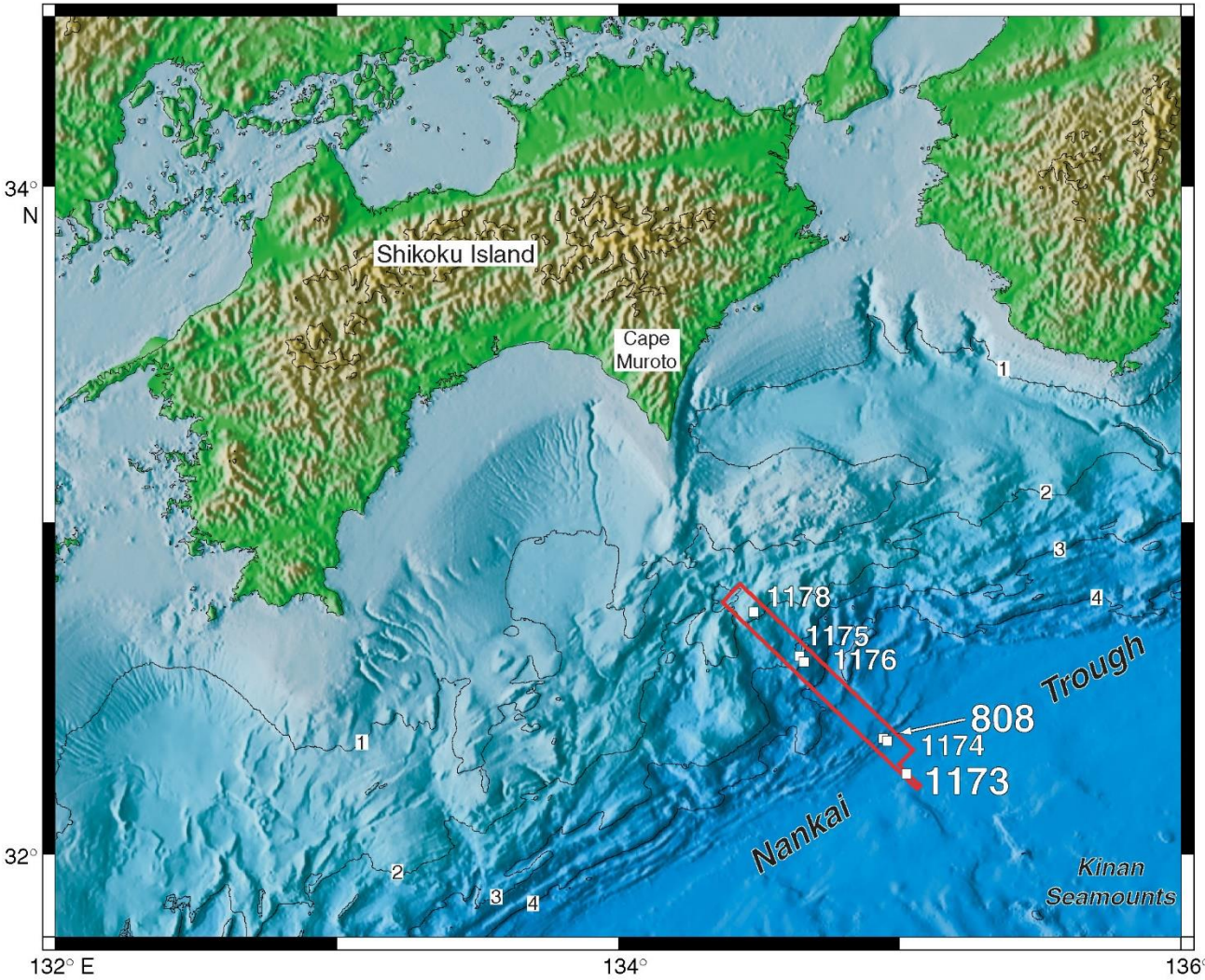

Shipboard Scientific Party, 2002. Chapter 1, Summary. In Proceedings of the ODP, Initial Reports, Leg 196

http://www-odp.tamu.edu/publications/196_IR/chap_01/chap_01.htm

Giappone (Nankai Trench)

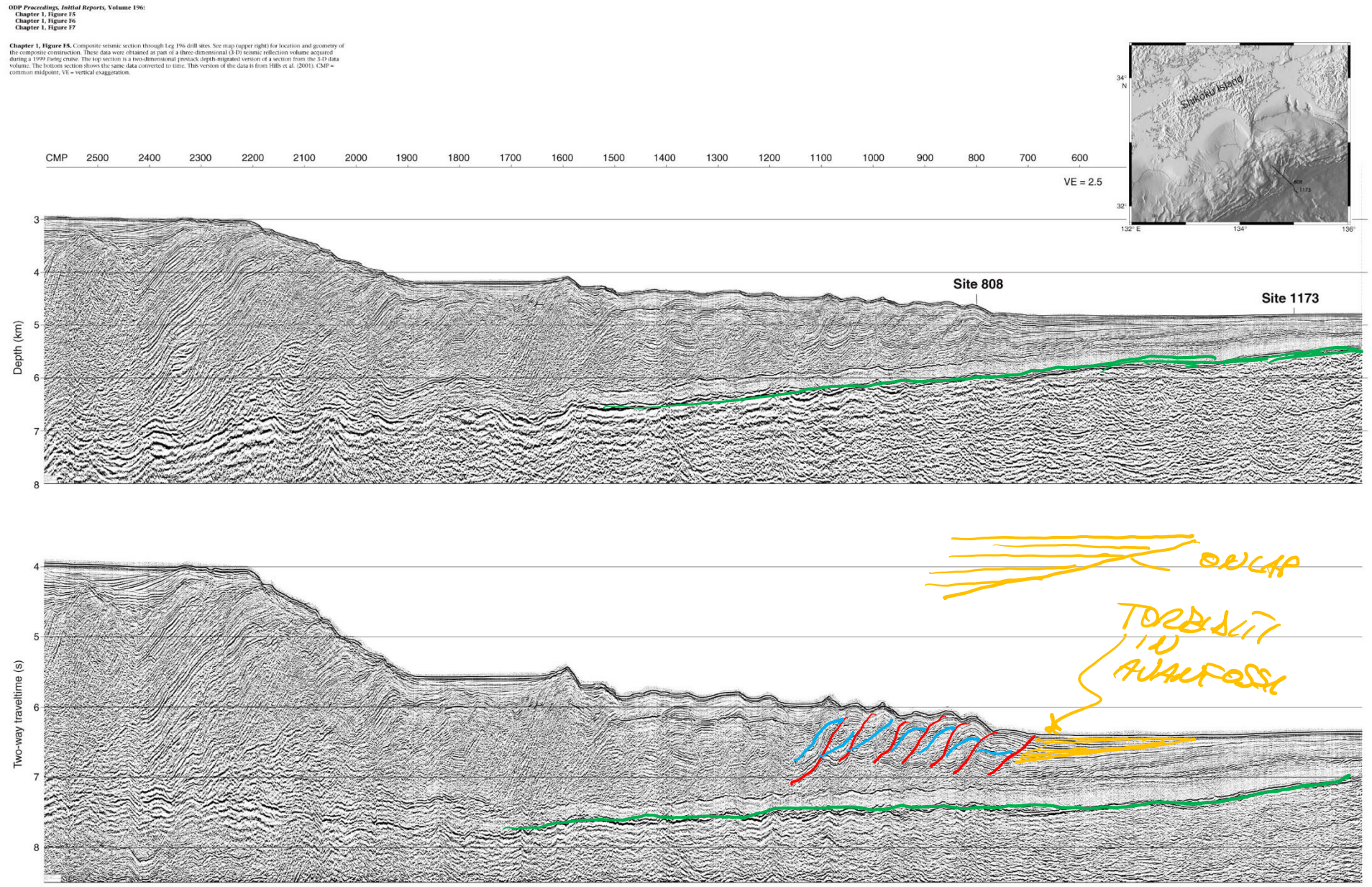

Mikada, H., Becker, K., Moore, J.C., Klaus, A., et al., 2002 Proceedings of the ODP, Initial Reports, Leg 196, 2002. Oversized Materials http://www-odp.tamu.edu/publications/196_IR/196TOC.HTM

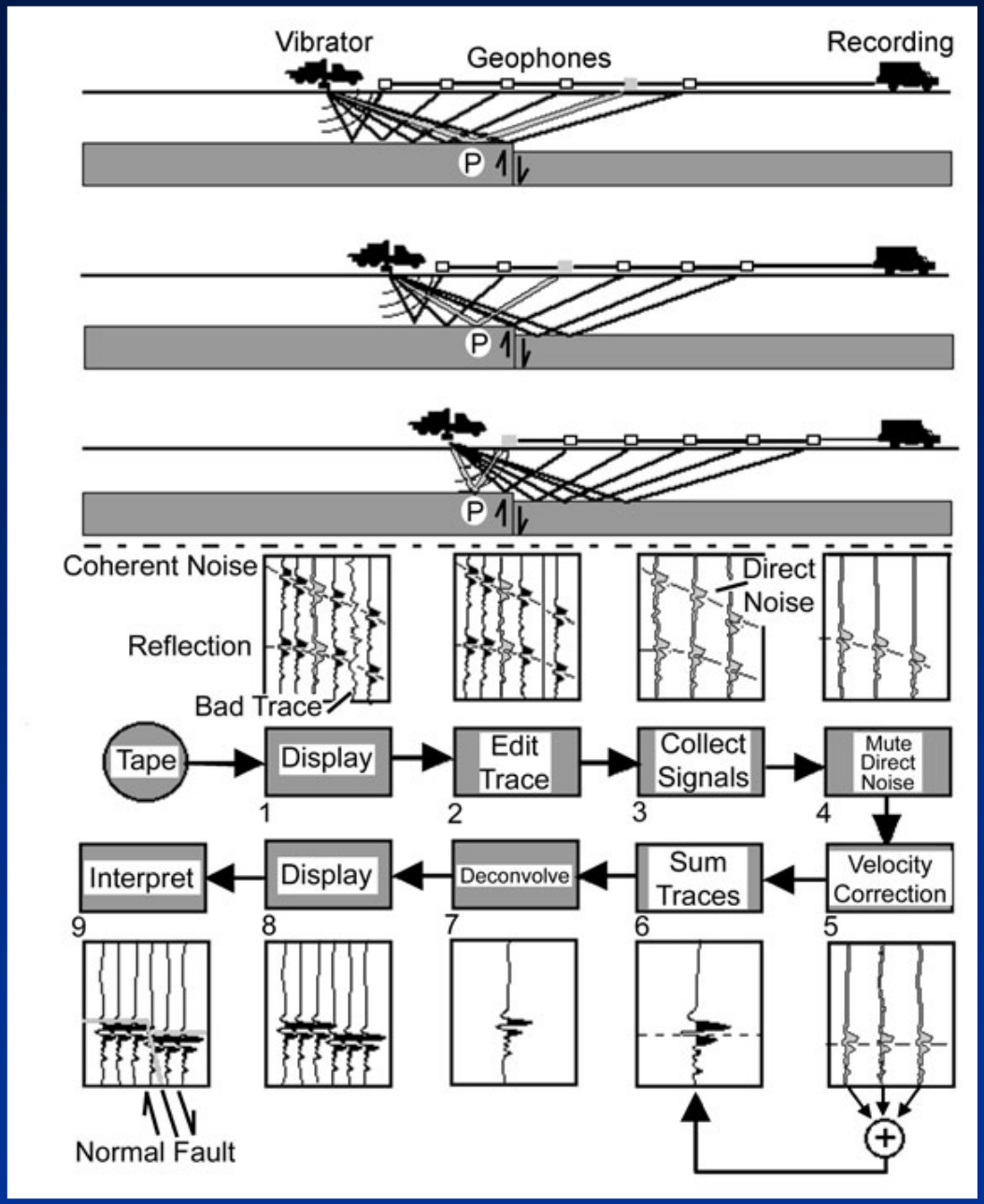

Da van der Pluim & Marshak, 2004

Figure F4. Seismic depth section across Sites 1173, 1174, and 808 (Hills et al., 2001). The section is composed of a northwest-trending segment of seismic line 215 through Site 1173, with a diagonal transition to line 281 that passes near Sites 1174 and 808. CDP = common depth point, VE = vertical exaggeration.

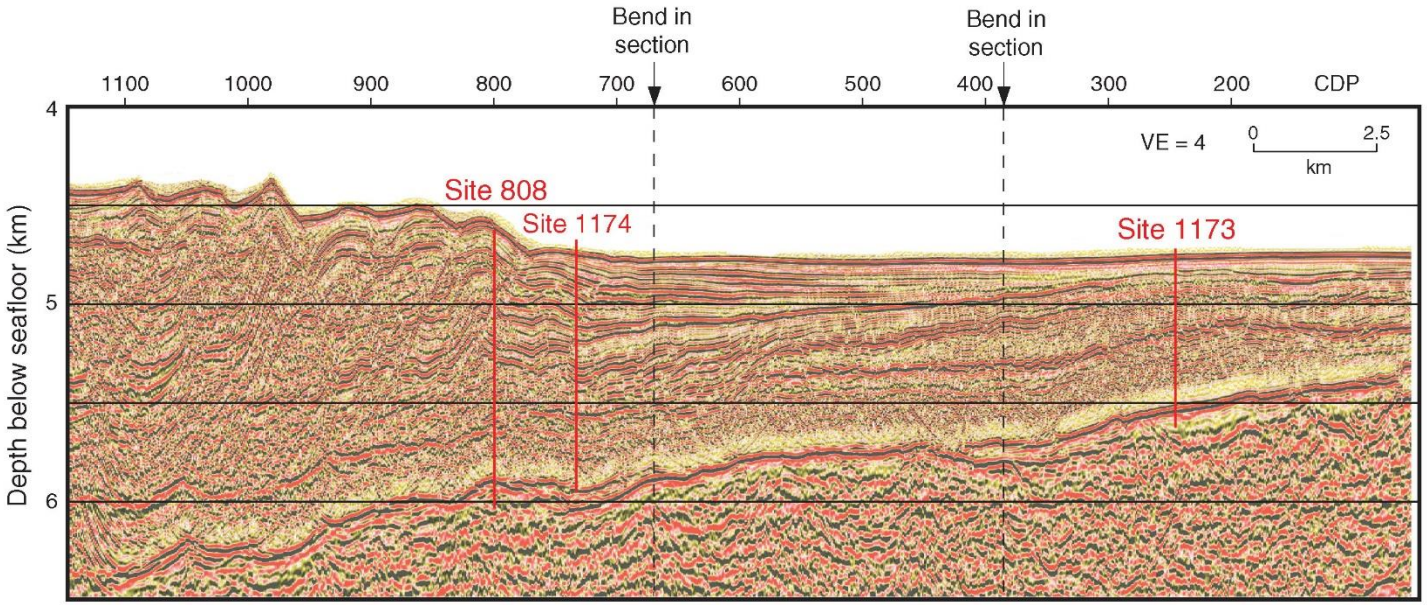

koku Basin to the imbricate thrust zone.
liagonal transition to line 281 that passes

Shipboard Scientific Party, 2002. Chapter 1, Summary. In Proceedings of the ODP, Initial Reports, Leg 196 http://www-odp.tamu.edu/publications/196_IR/chap_01/chap_01.htm

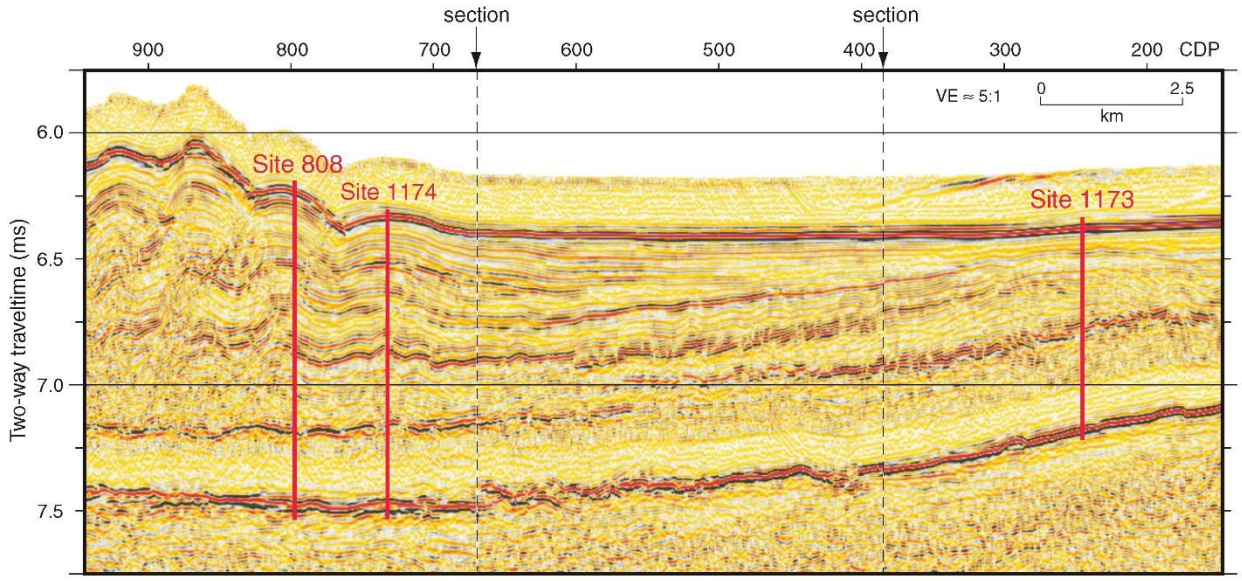

Giappone (Nankai Trench)

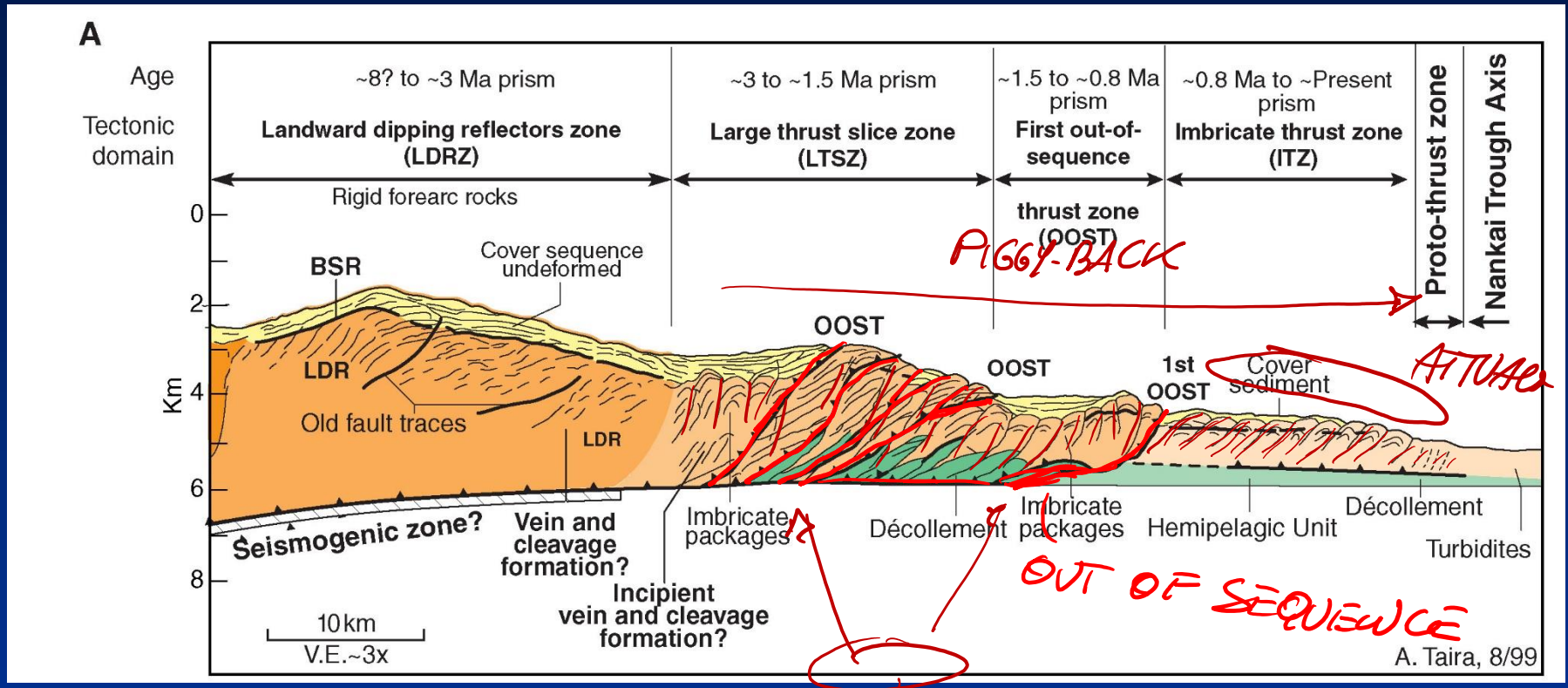

Moore, Taira, Baldauf & Klaus, 2000, ODP Scientific Prospectus Leg 190
http://www-odp.tamu.edu/publications/prosp/190_prs/190toc.html

OUT OF SEQUENCE E THRUST ESTERNI
DELL'OFFSCRAPING SONO COEVI

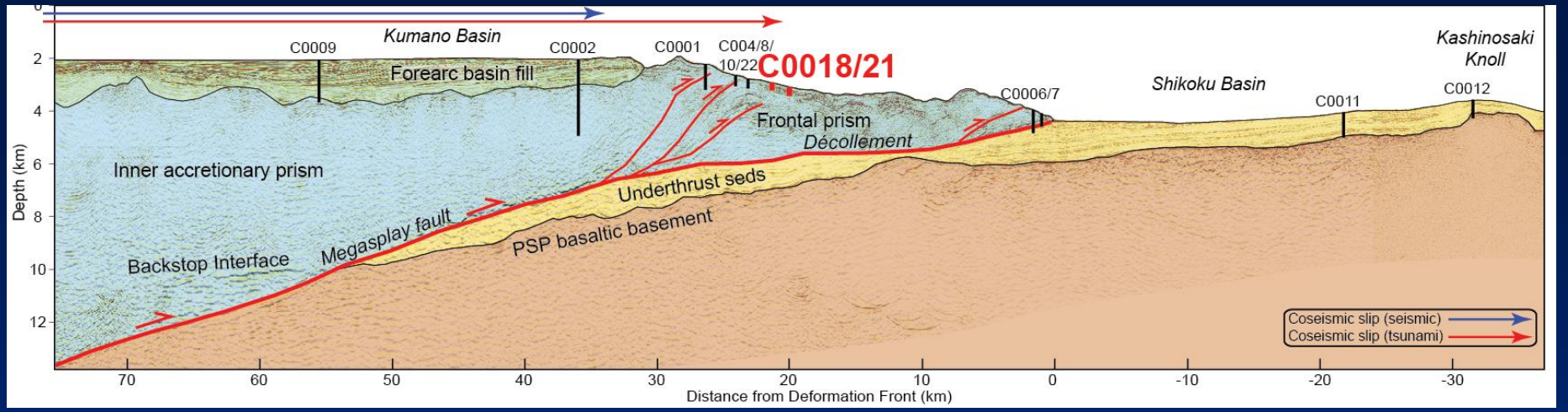

Moore et al., 2014

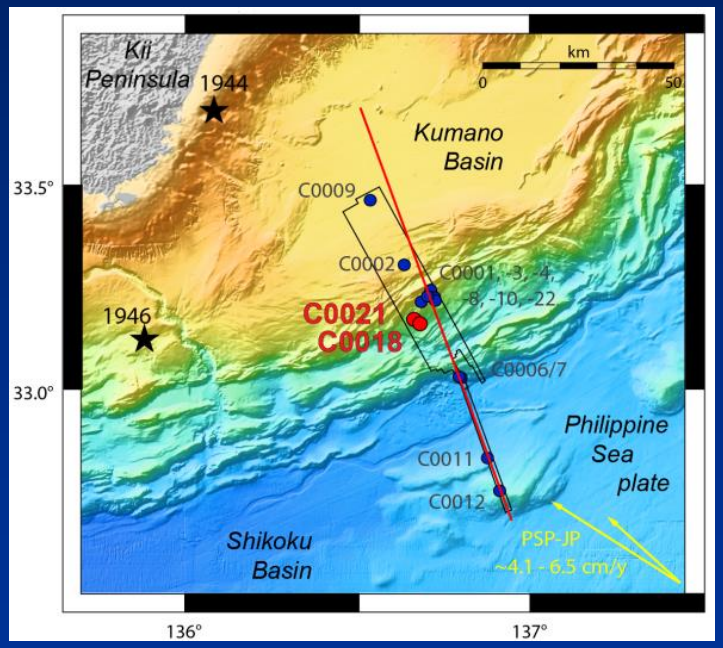

Moore et al., 2014

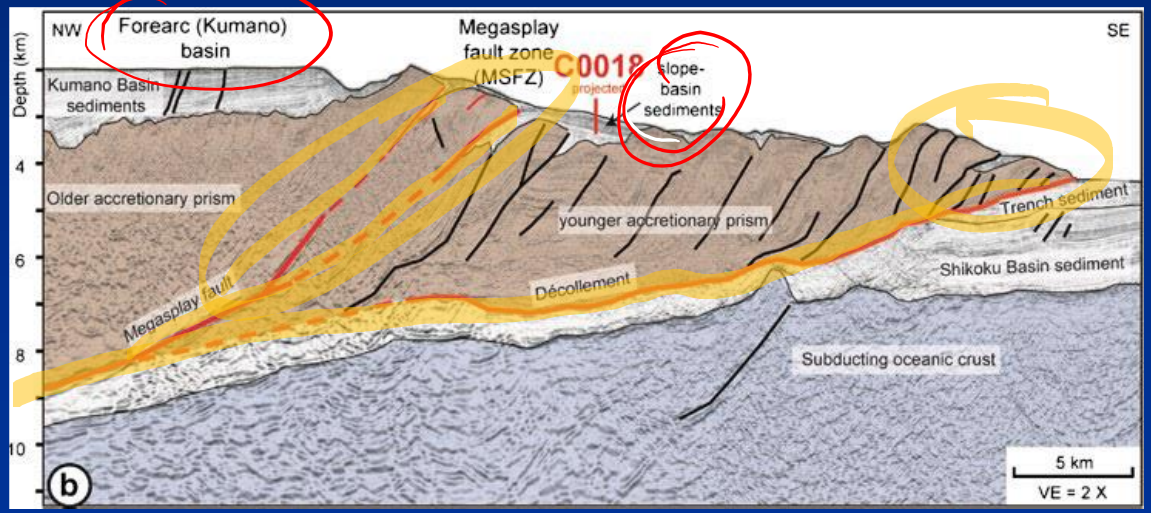

Strasser et al., 2012

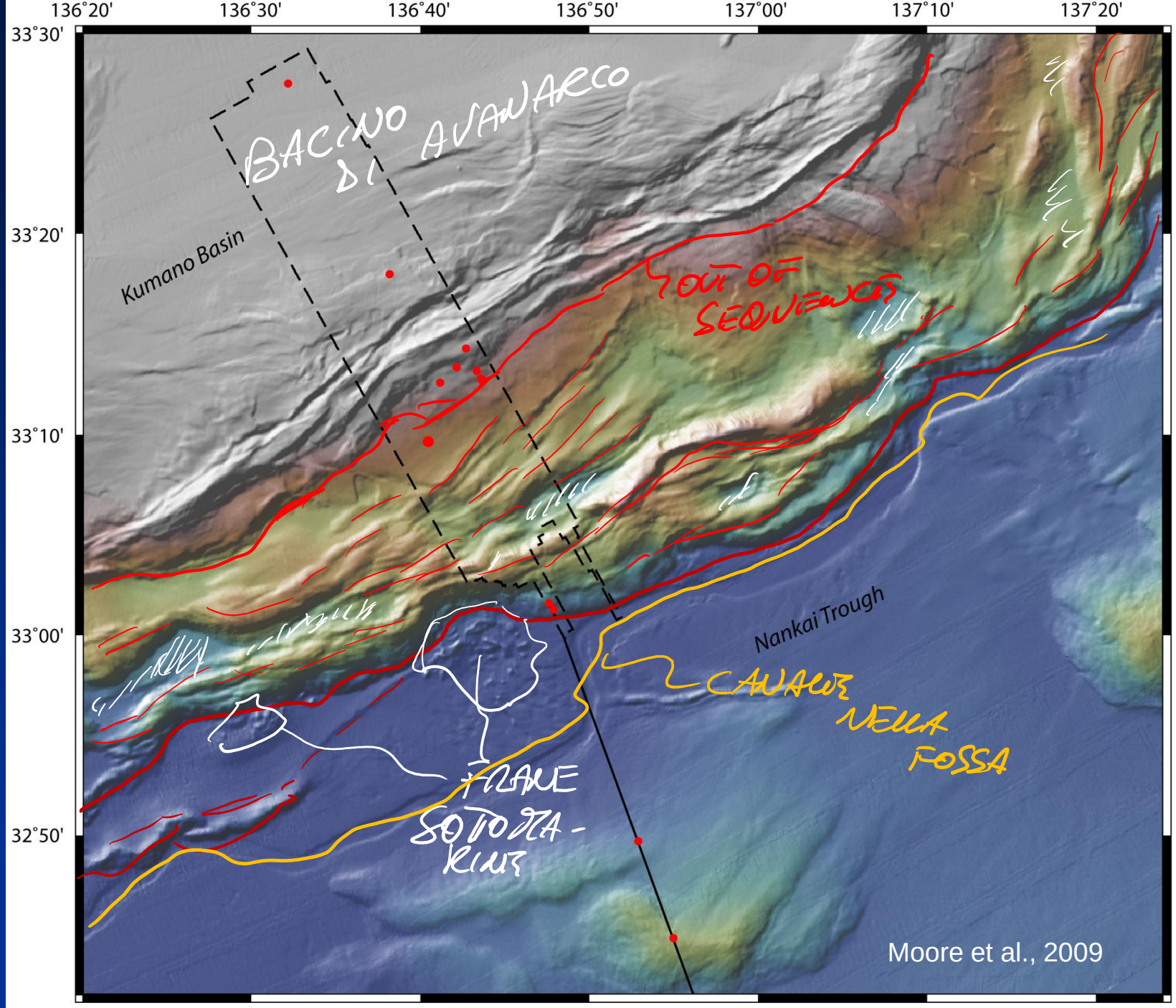
136°20'
136°30'
136°40'
136°50'
137°00'
137°10'
137°20'
33°30'
33°20'
33°10'
33°00'
32°50'
BACINO DI AVANARCO
Kumano Basin
FOUT OF SEQUENCES
Nankai Trough
CANALE NELLA FOSSA
FIANCO SOTTOSTANTE
Moore et al., 2009

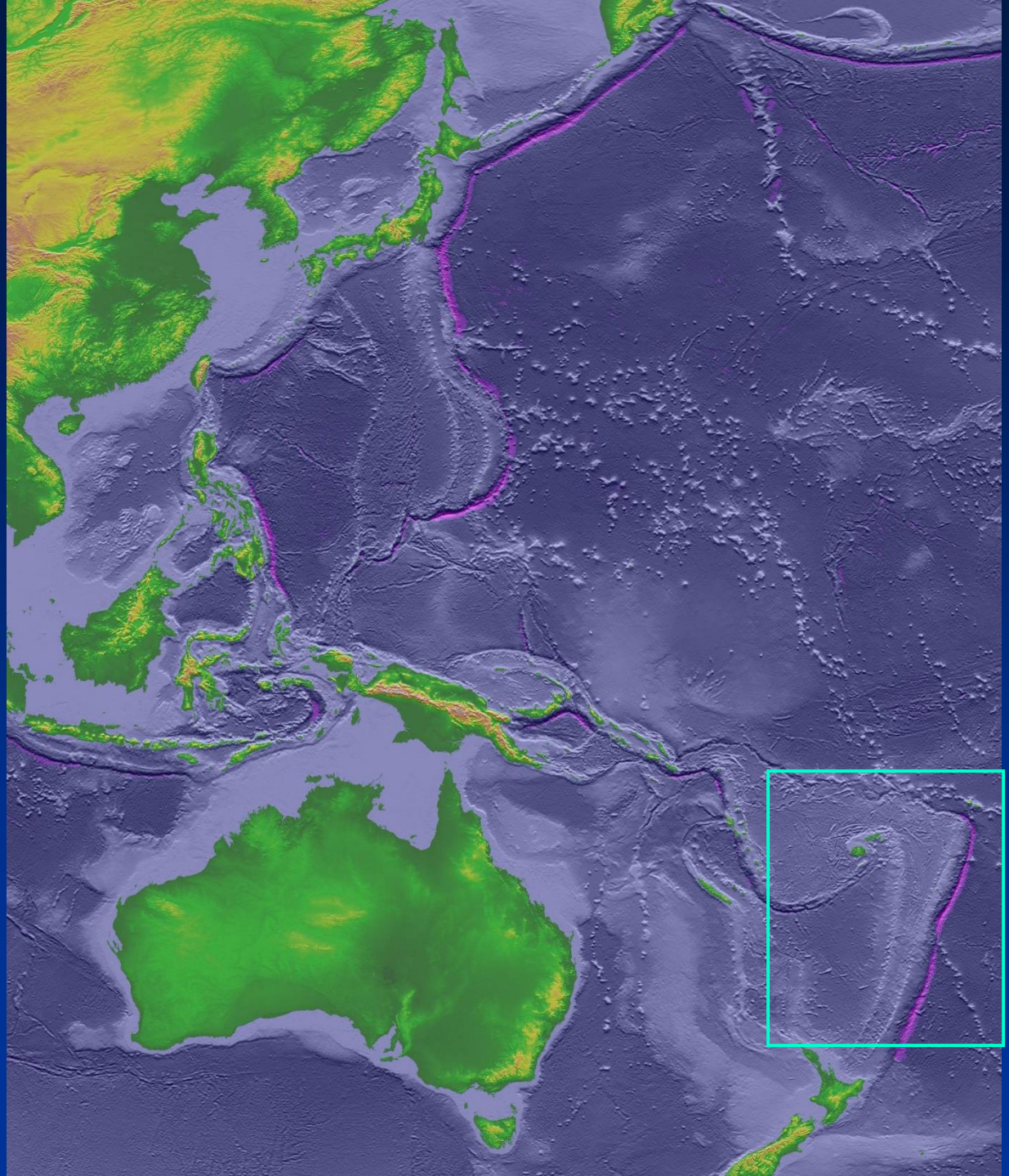

Shaded reliefs e batimetria da NOAA National Centers for Environmental Information (NCEI)

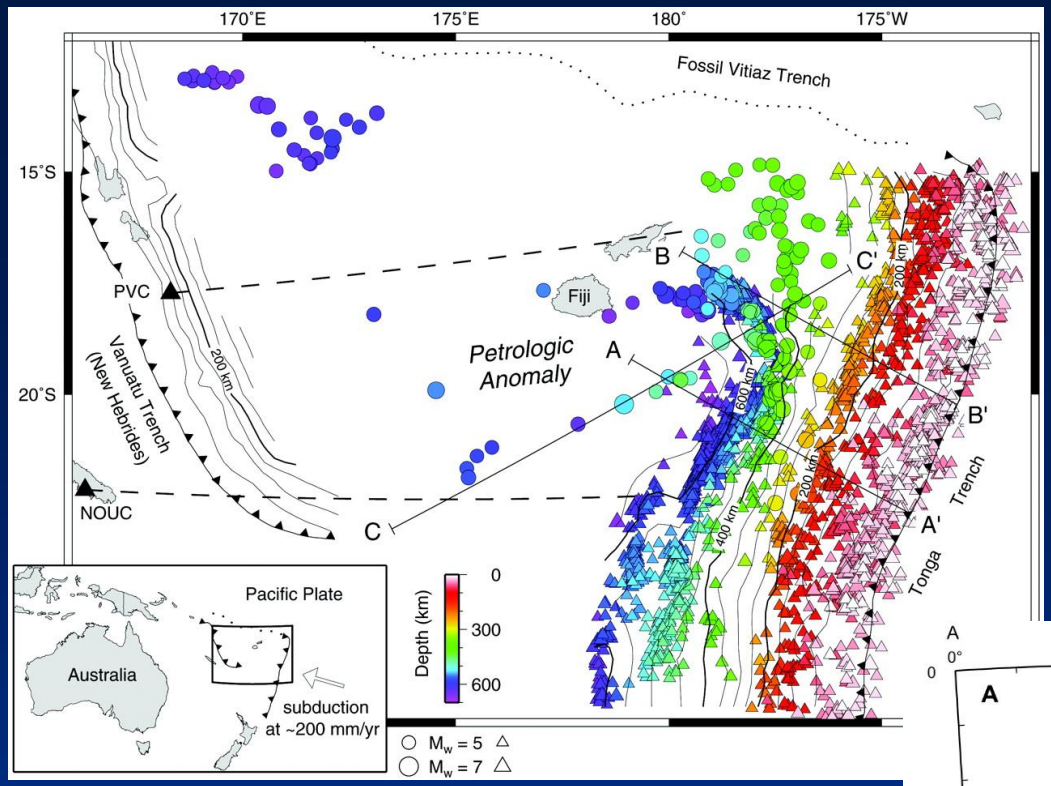

Da Cheng & Brudzinski, 2001

Mappa e tre sezioni crostali-mantelliche mostranti la profondità degli ipocentri dei terremoti a magnitudo ≥ 5 occorsi tra il 1964 e il 1999 nelle Tonga Fiji.

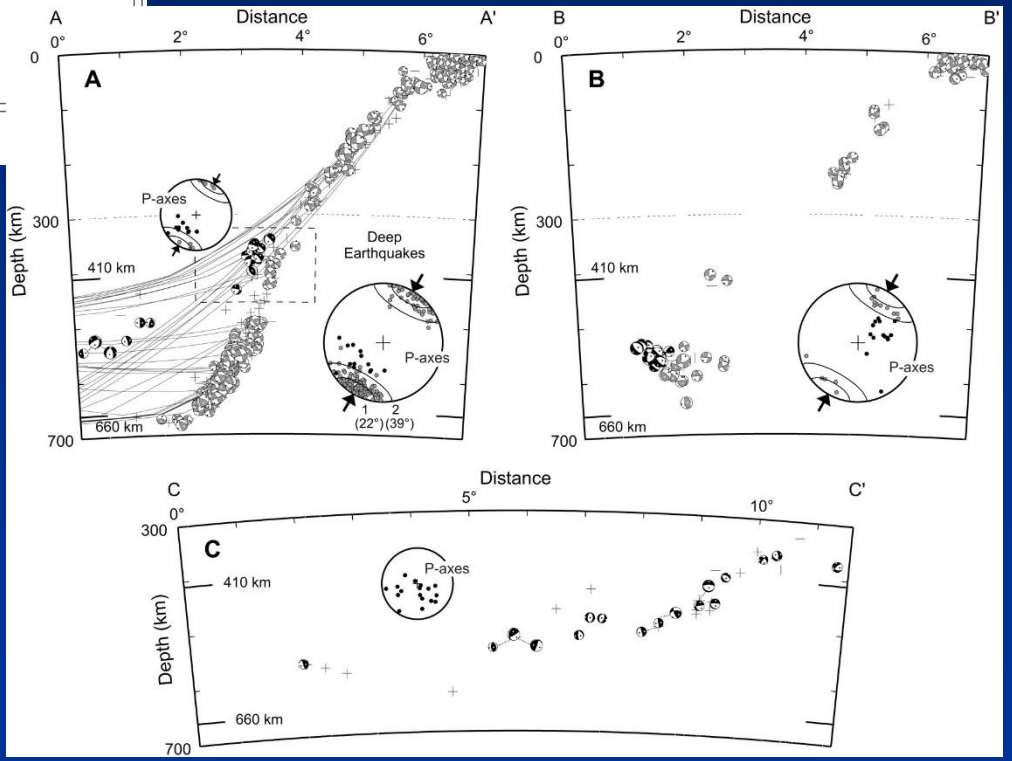

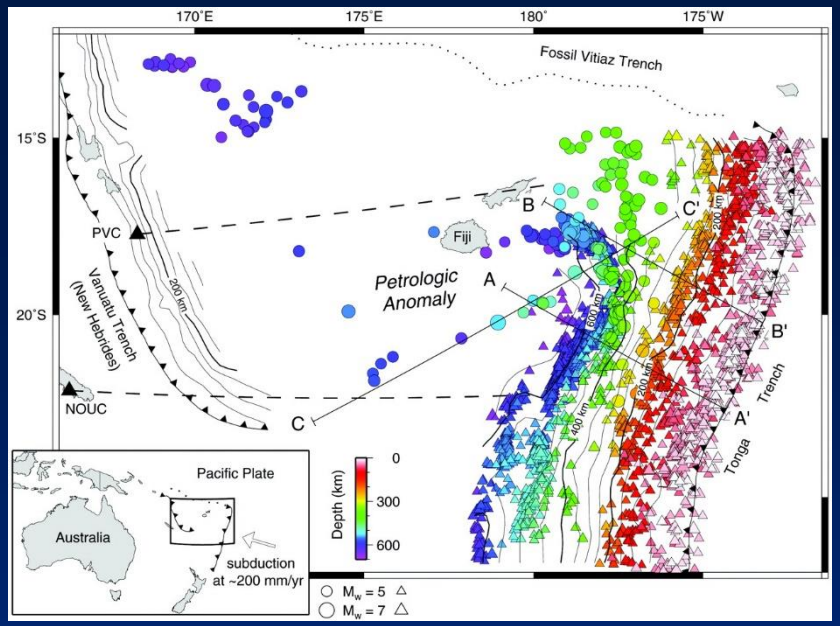

Ricostruzione 3D della sismicità sotto alla fossa-retroarco di Tonga

Da Cheng & Brudzinski, 2001

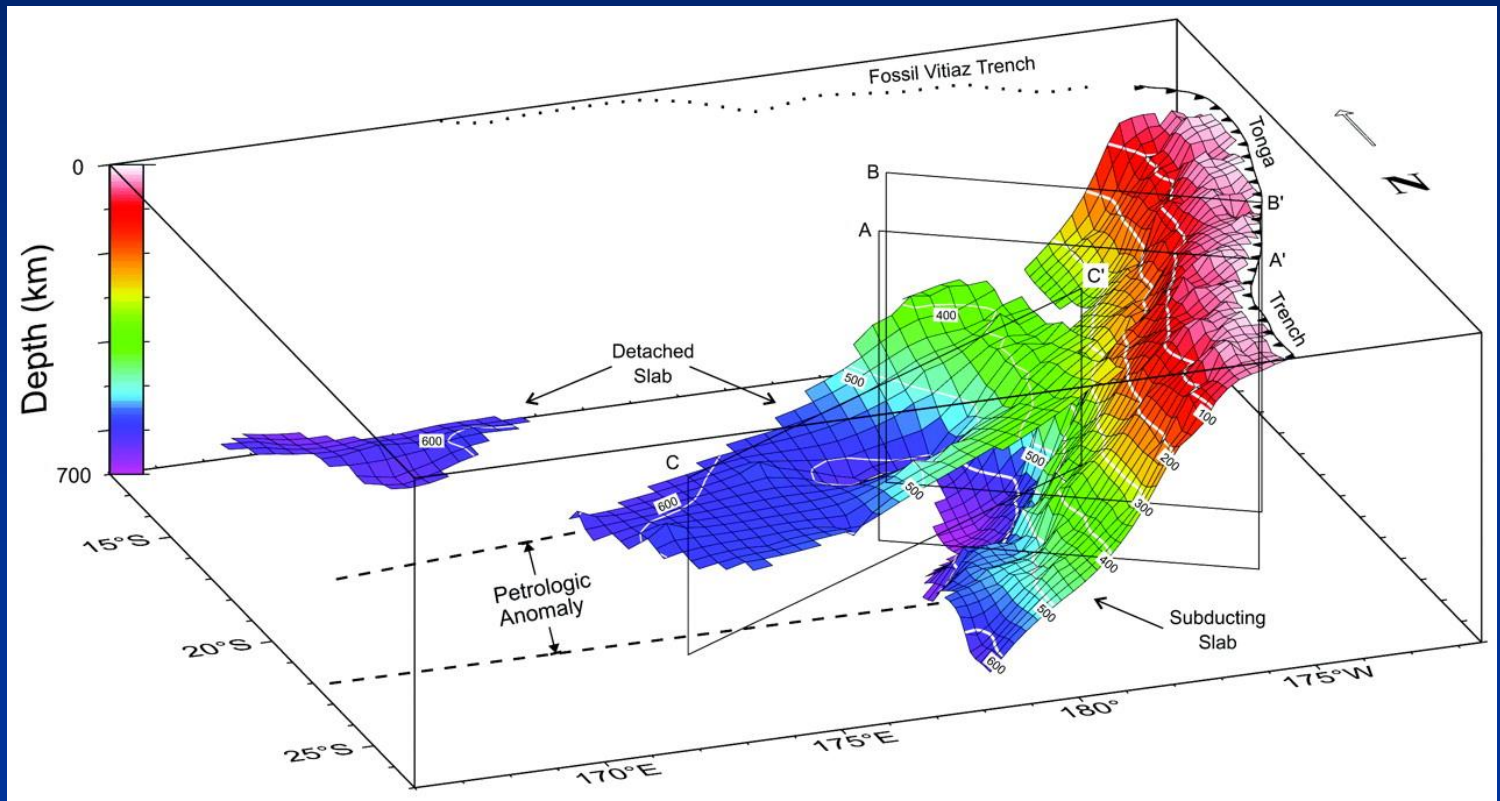

Prismi di accrezione: cordillera-andino

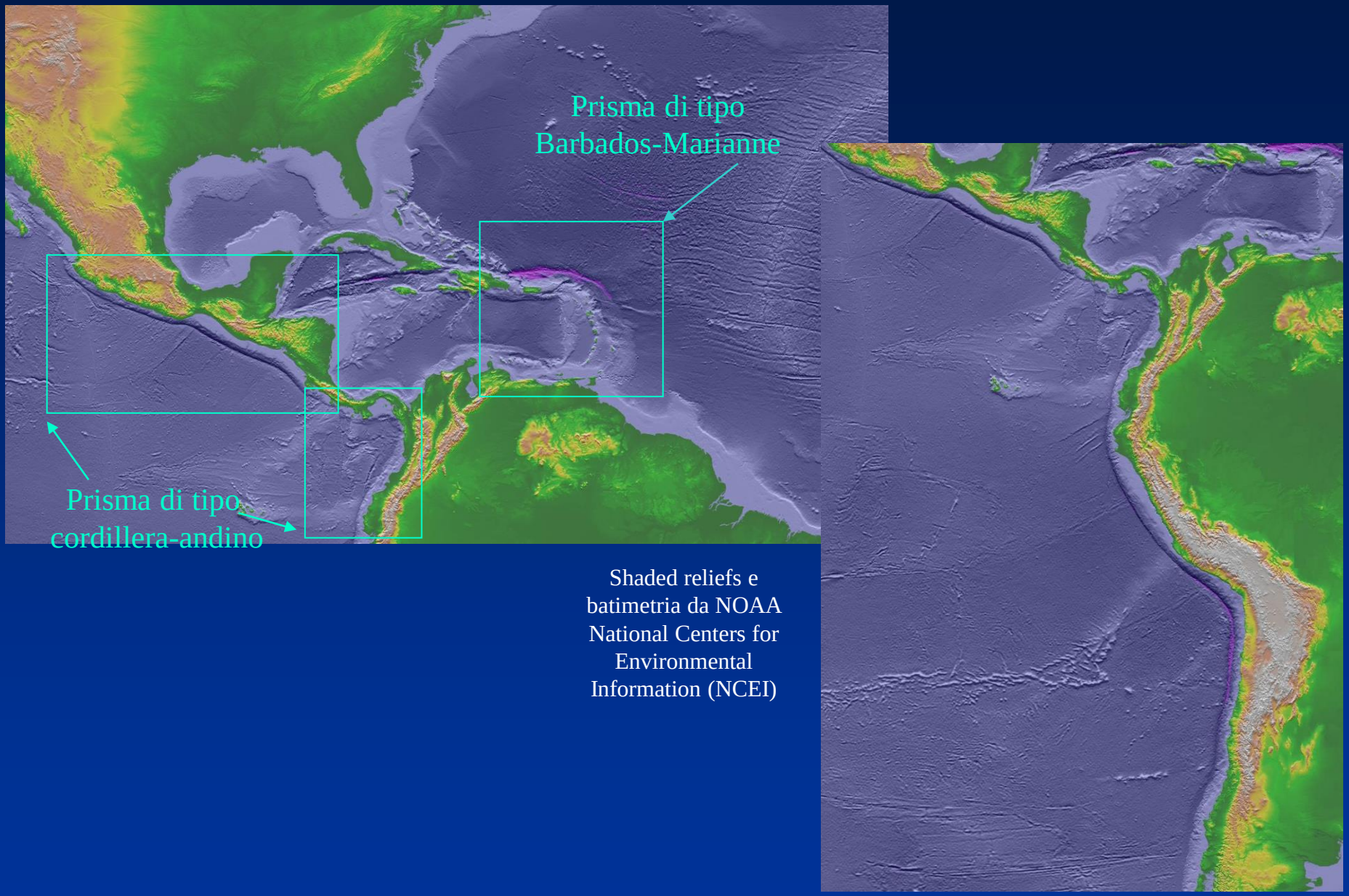

Shaded reliefs e batimetria da NOAA National Centers for Environmental Information (NCEI)

Shaded reliefs e batimetria da NOAA National Centers for Environmental Information (NCEI)

Prismi di accrezione

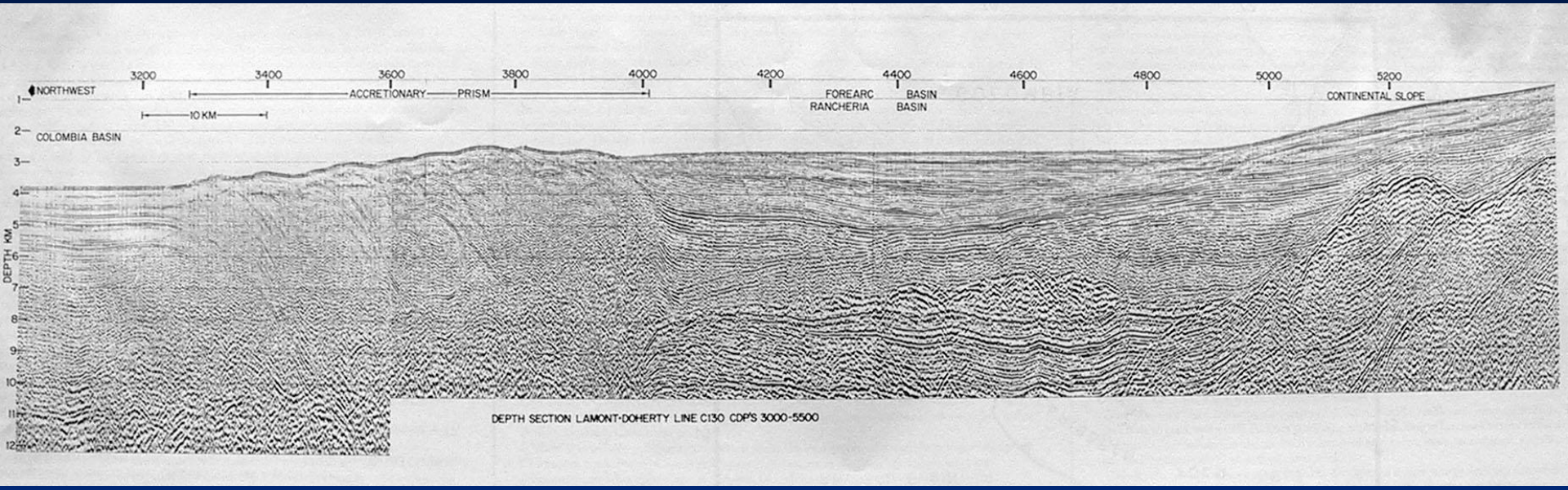

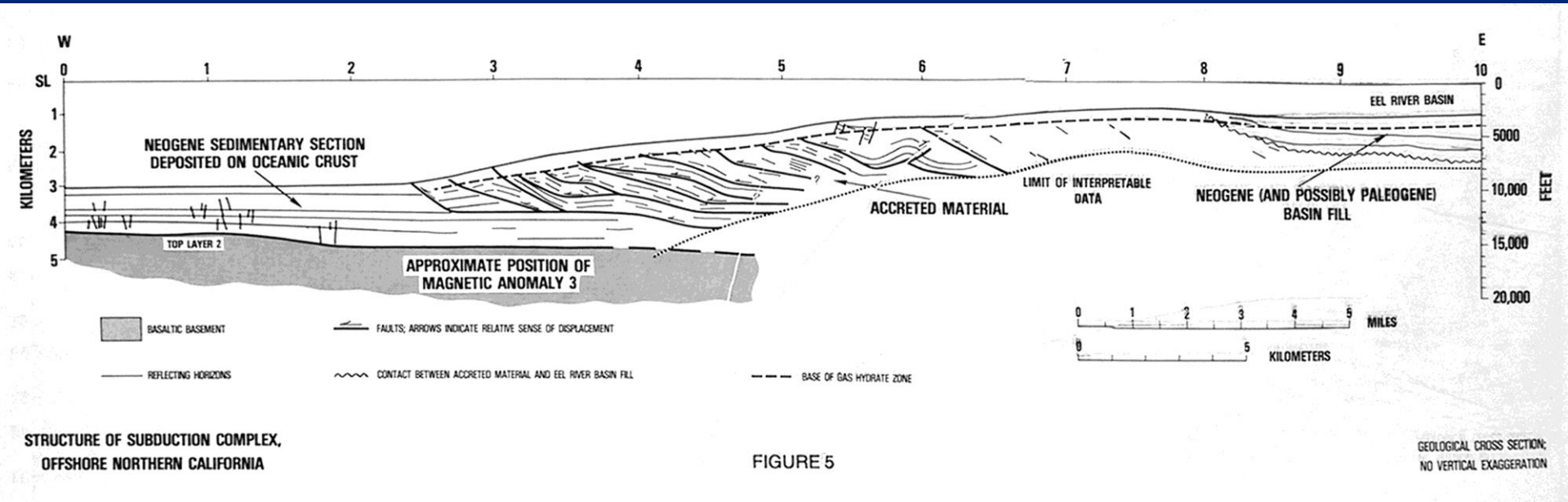

STRUCTURE OF SUBDUCTION COMPLEX, OFFSHORE NORTHERN CALIFORNIA

FIGURE 5

GEOLOGICAL CROSS SECTION; NO VERTICAL EXAGGERATION

Tipo cordillera o andino

Da Bally (ed.), 1985

Prismi di accrezione

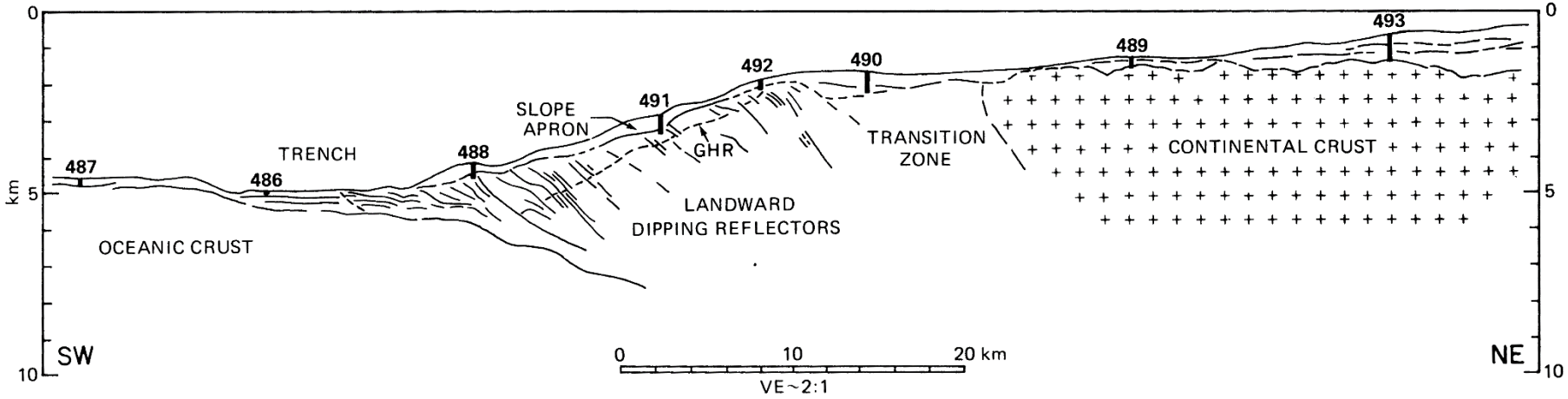

Figure 7. Cross section across the Middle America Trench off Southern Mexico in the Leg 66 drilling area (Moore and others, 1982). Vertical exaggeration (VE) is about 2:1.

Da Moore & Lundberg, 1986

Tipo cordillera o andino

https://commons.wikimedia.org/wiki/File:Tectonic_plates_boundaries_detailed-en.svg

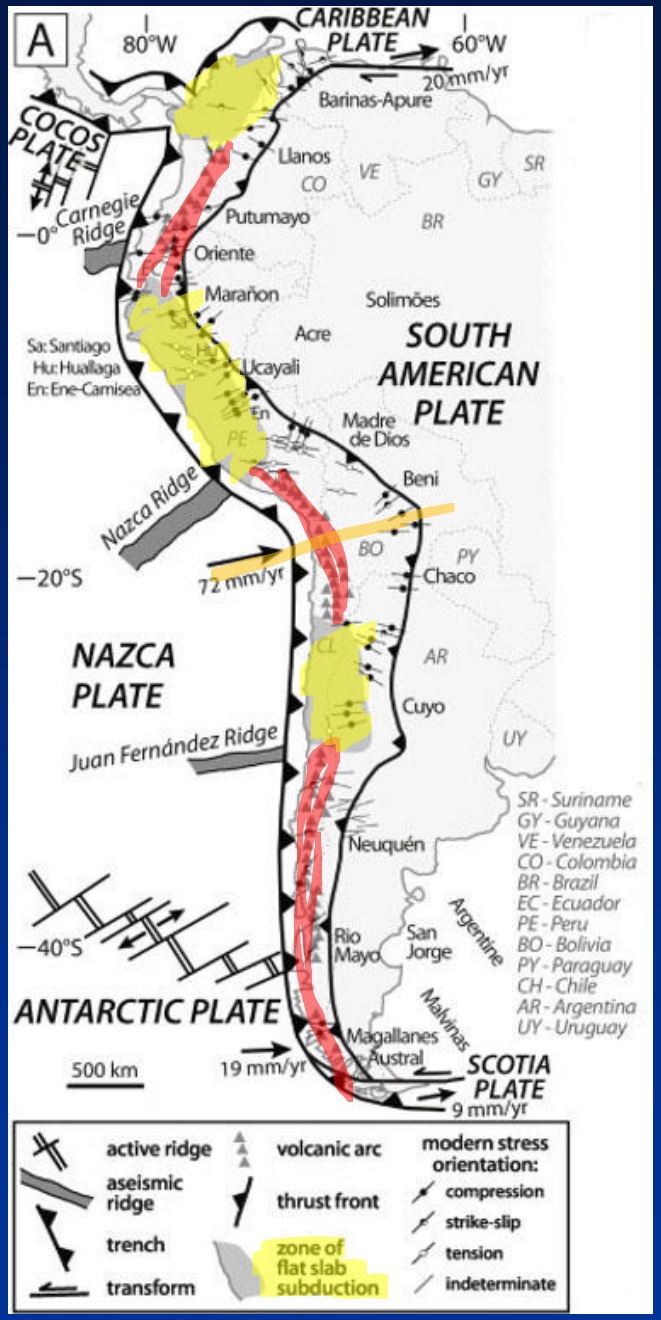

Da Horton, 2018

Da Armijo et al., 2015

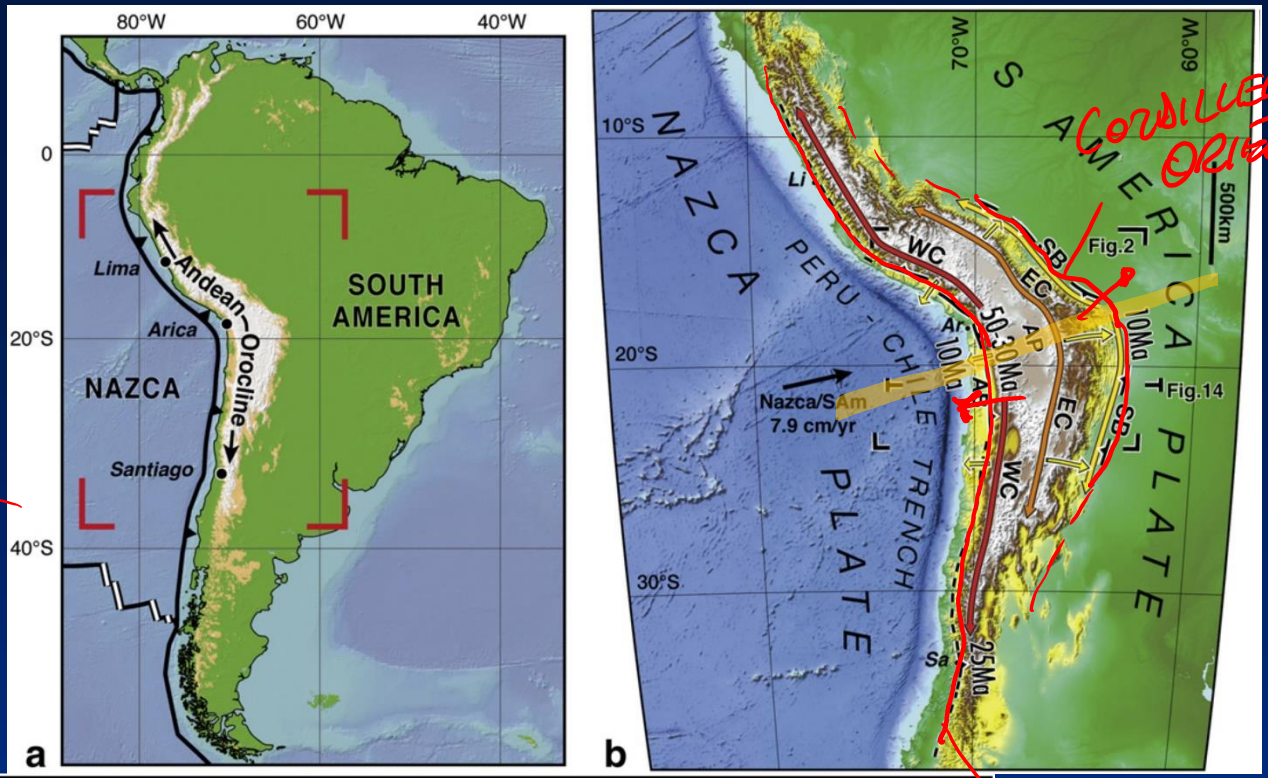

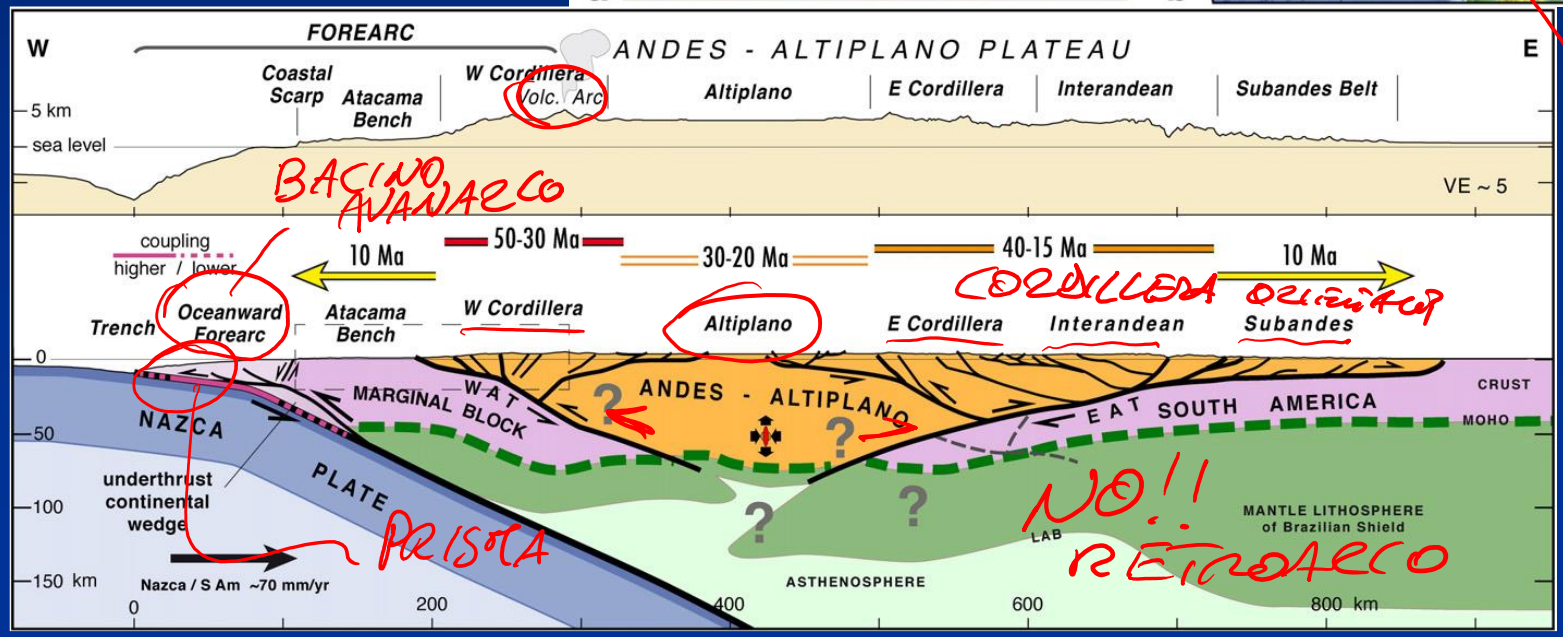

Da Armijo et al., 2015

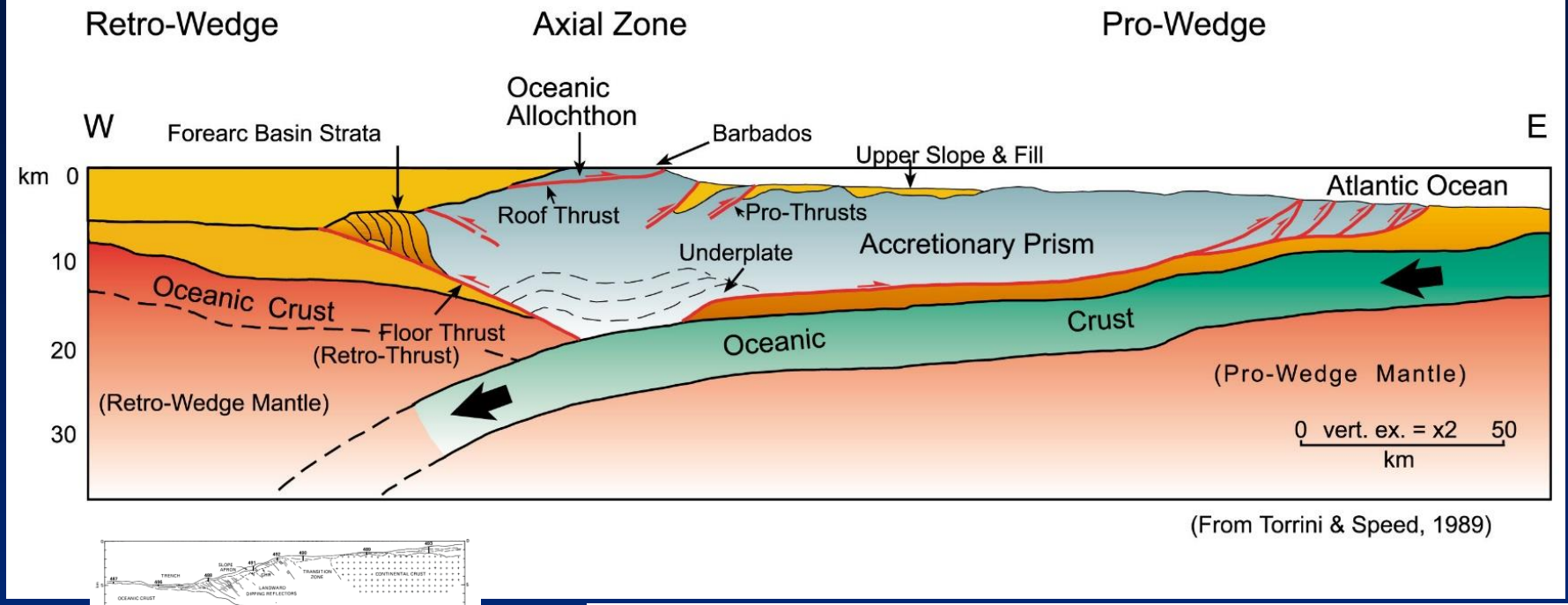

Da Armijo et al., 2015; Moore and Lundberg, 1986

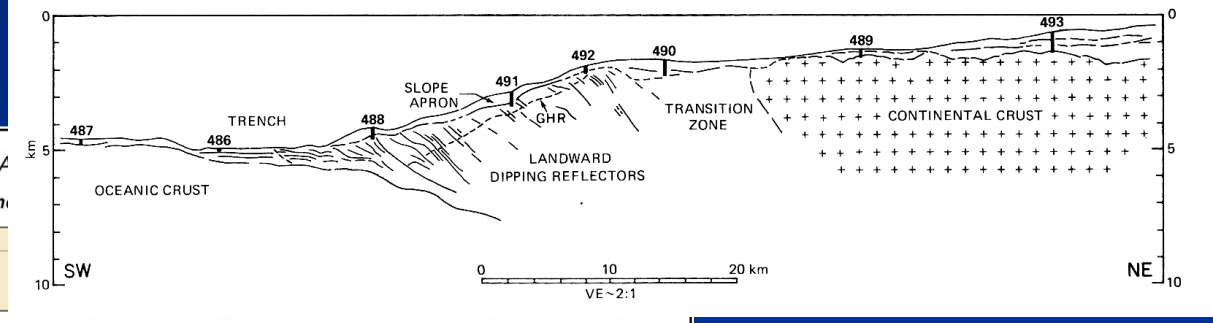

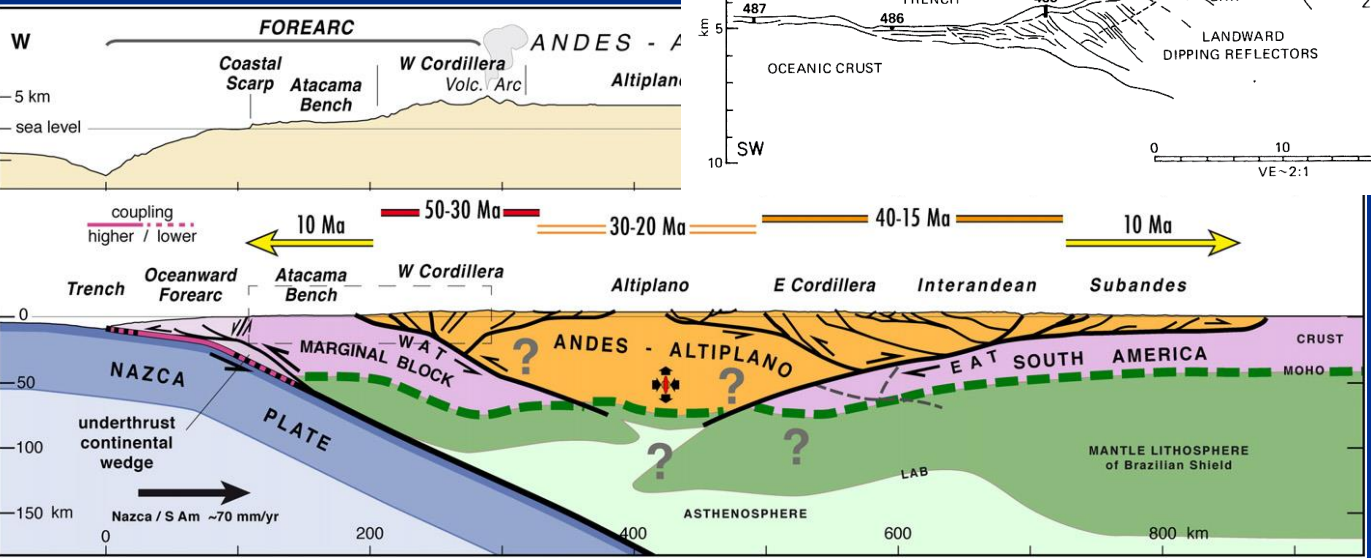

Prismi di accrezione: i due tipi

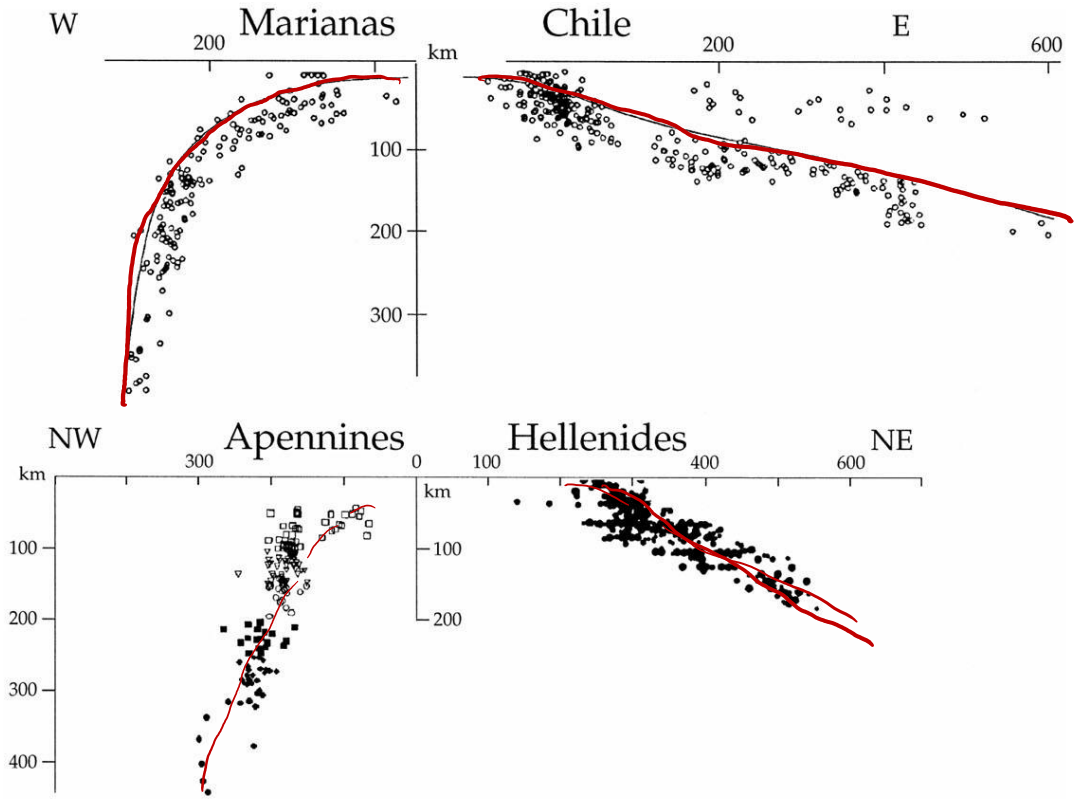

Fig. 3. Ipocenters of the Marianas and Chile subduction zones in the Pacific (after Isacks and Barazangi, 1977), compared with the seismicity of the Apennines (Selvaggi and Chiarabba, 1995) and Hellenides (Papazachos and Comninakis, 1977) opposed subduction zones. The Pacific asymmetry is present also in the central Mediterranean subduction zones where the Ionian oceanic lithosphere is subducting contemporaneously both underneath the Apennines and the Hellenides. Location of the sections in Fig. 2.

Da Doglioni et al., 1999

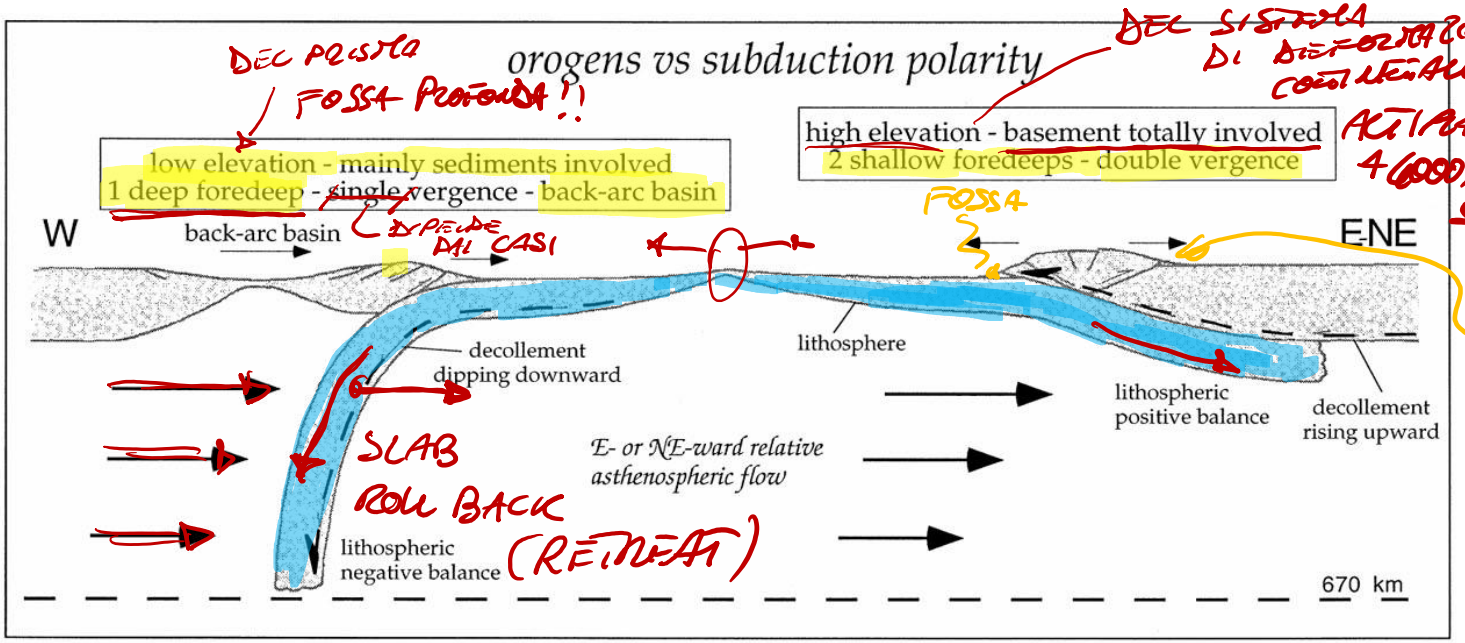

Fig. 5. W-directed subduction zones are steeper and deeper with respect to the E–NE- or NNE-directed subduction zones. Note that the decollement plane of the eastern plate is warped and subducted in case of W-directed plane, whereas it ramps toward the surface in the E–NE-directed subduction, enabling the uplift of deep seated rocks: this asymmetry may be explained by the 'westward' drift of the lithosphere relative to the mantle and controls the strong differences in morphology, structure and lithology of the related thrust belts.

Da Doglioni et al., 1999

Active Back-Arc Basins (BAB) of the World

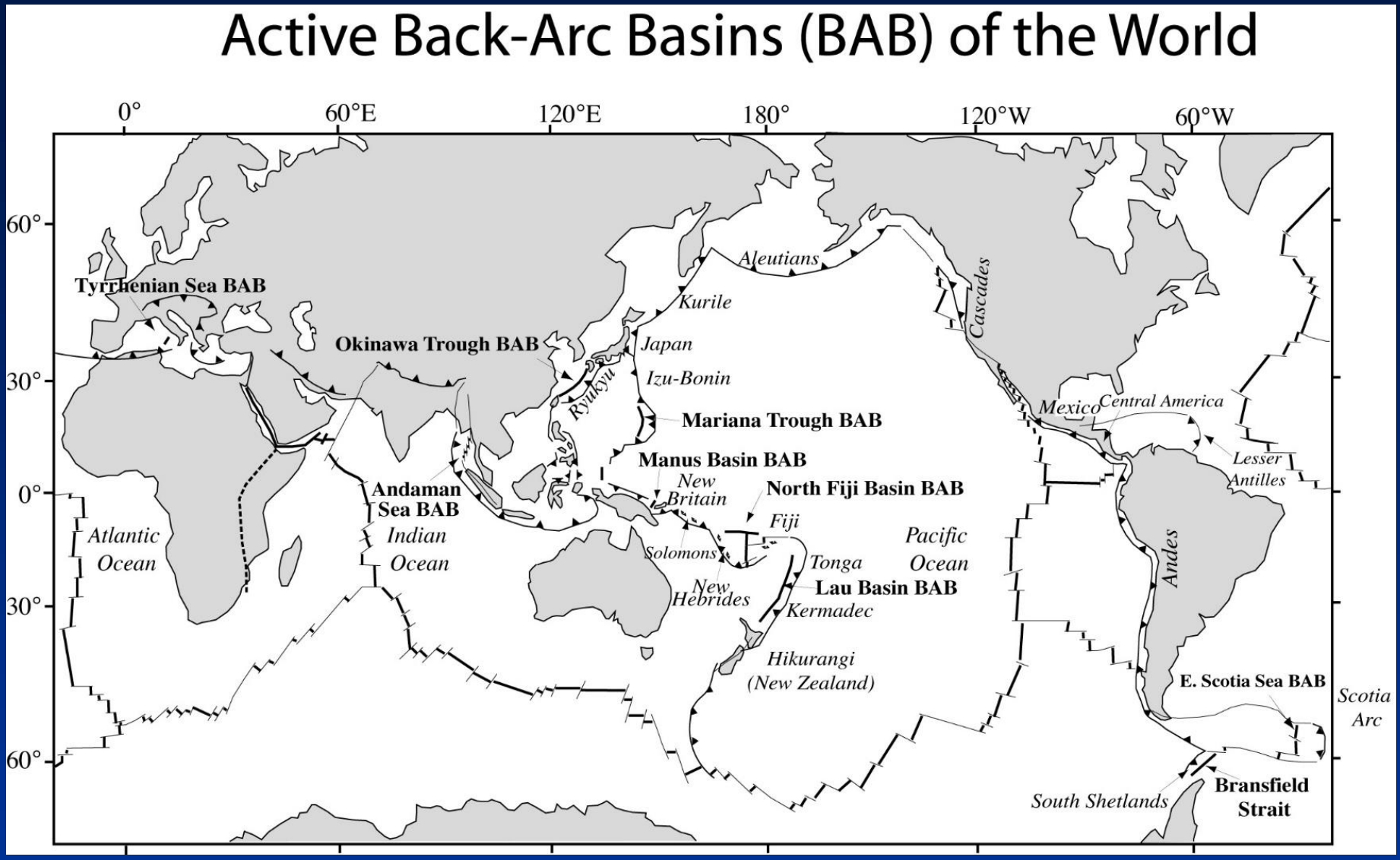

Da Wikipedia e da Guinot & Segonzac, 2017

Foreland system: flessura della litosfera

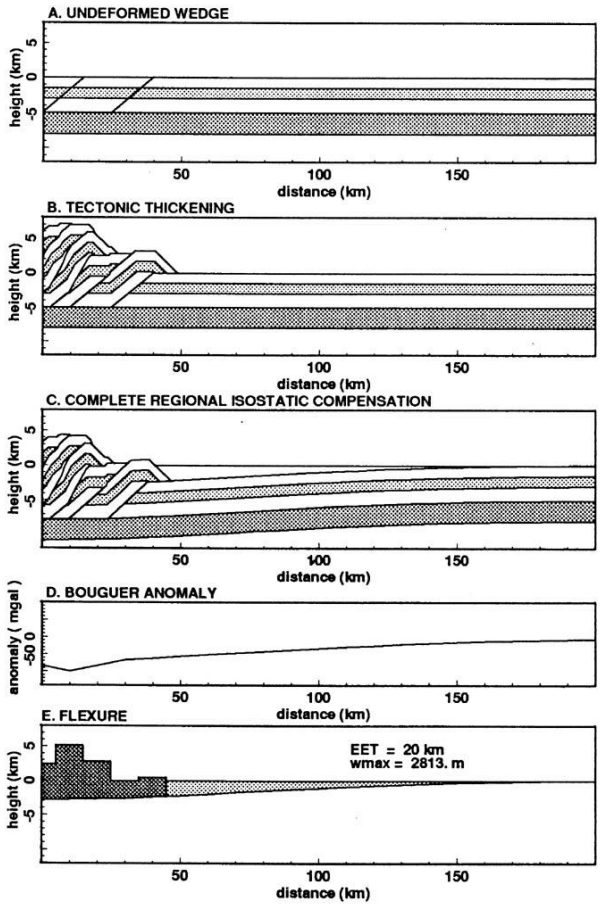

Figure 2-1. Effect of thrust loading on lithospheric response. Regional isostasy results in depression filled with sediments, a) initial situation, b) emplacement of thrust sheets onto the craton, c) flexural response to thrust mass loading, d) associated Bouguer gravity anomaly, e) flexure in (c) calculated with thrust load and sediment load on lithosphere with 20 km effective elastic thickness (EET), quantified after Price [1973].

Da Zoetemeijer, 1993

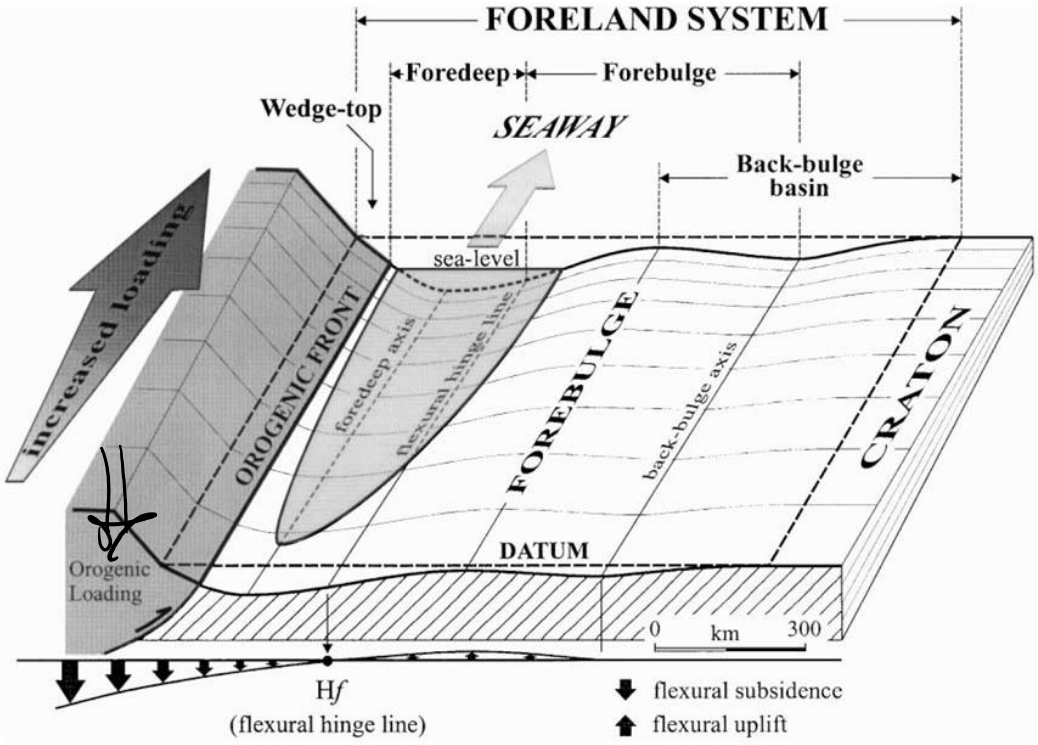

Fig. 3. Configuration of the foreland system during orogenic loading with strike variability. The magnitude of the flexural deflection is proportional to the degree of loading. Four depozones may be differentiated, i.e. wedge-top, foredeep, forebulge and back-bulge. We refer to the wedge-top and foredeep as the proximal sector, and to the forebulge and back-bulge as the distal sector. The proximal and distal sectors of the foreland system are separated by the flexural hinge line. The topographic elevation of the adjacent craton, approximated with a horizontal plane, is taken as a datum. The base-level of deposition within the foreland system may be in any position (below, above or superimposed) relative to the datum, although surface processes on the craton (sedimentation, erosion) tend to adjust the datum to the base-level.

Da Catuneanu et al., 2000

Cunei sedimentari sin-tettonici: la Pianura padana

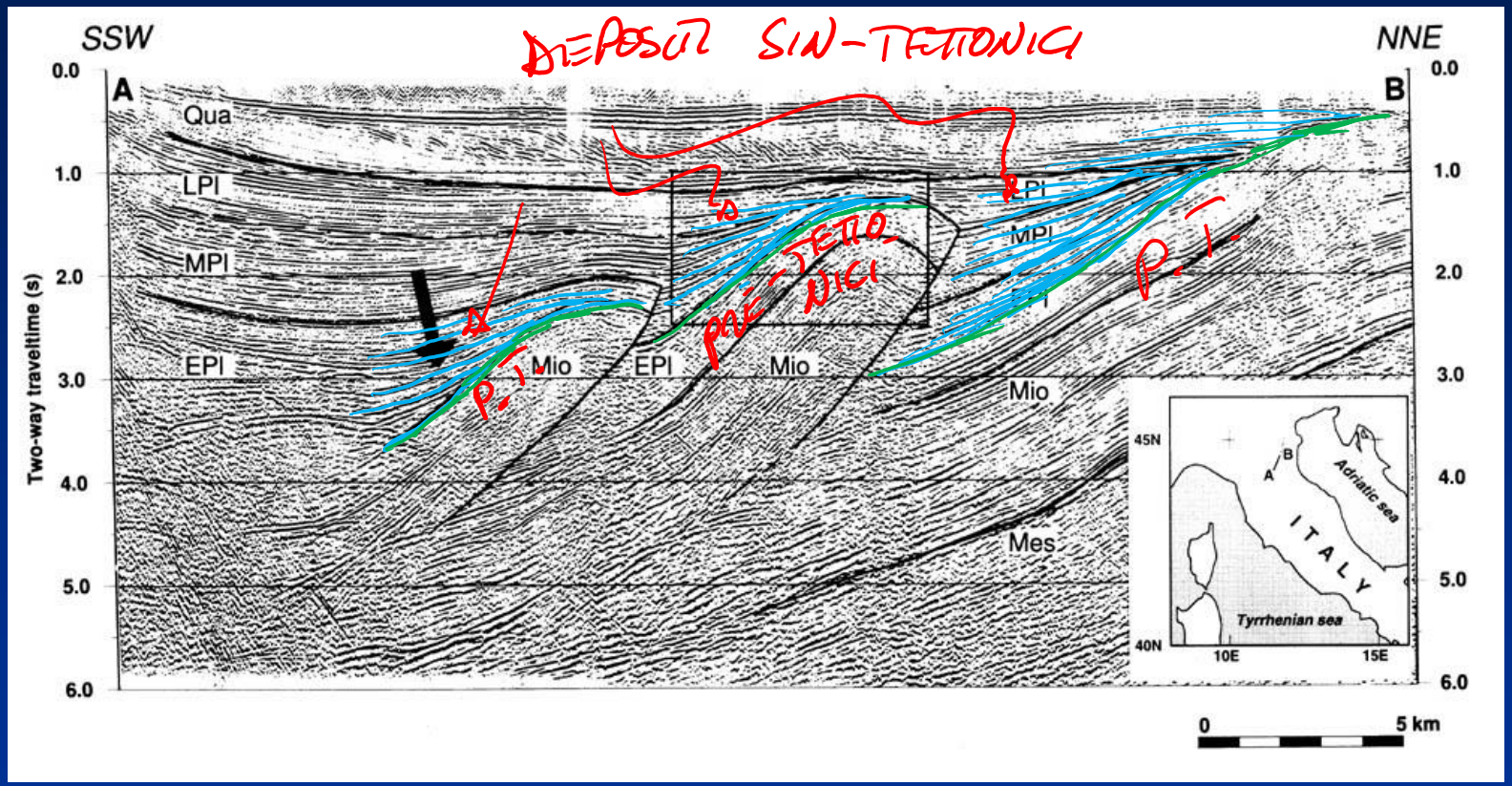

Da Zoetemeijer, 1993

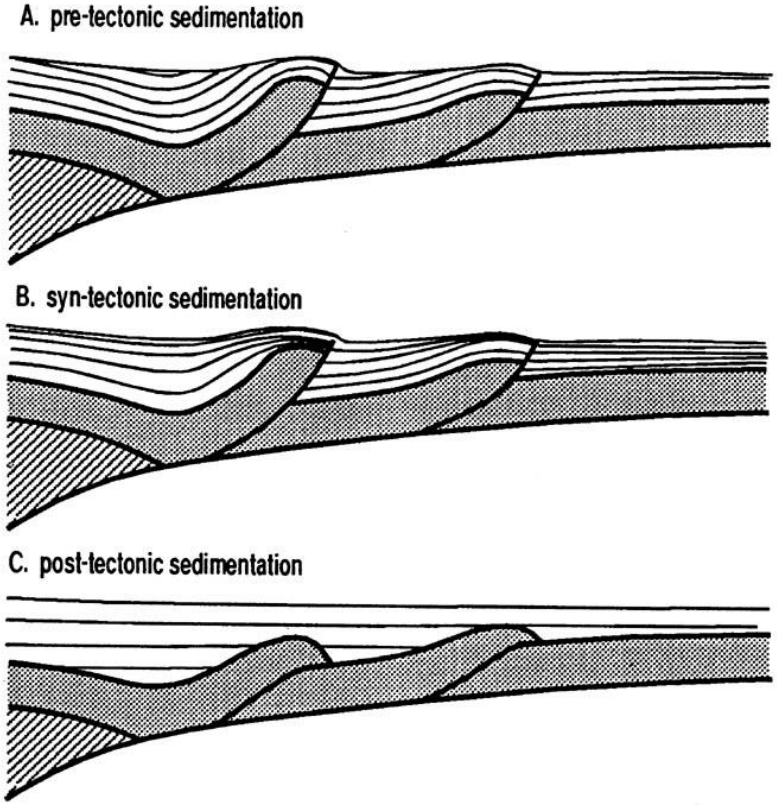

Figure 4-2. Schematic representation of possible basin configurations with sediment deposition (a) before, (b) during, and (c) after thrust interference (modified from Ricci Lucchi, 1986).

Da Zoetemeijer, 1993